Attachment 11

CHLE-019: Test Results for Chemical Effects Tests Stimulating Corrosion and Precipitation (T3 & T4)

PROJECT DOCUMENTATION COVER PAGE

Document No: CHLE-019	Revision: 2	Page 1 of 44
Title: Test results for chemical effect tests stimulating corrosion and precipitation (T3 &T4)		
Project: Corrosion/Head Loss Experiment (CHLE) Program		Date: Sept 23, 2013
Client: South Texas Project Nuclear Operating Company		

Summary/Purpose of Analysis or Calculation:

This report presents the results of tests that were conducted to validate the conclusions of medium-break LOCA and large-break LOCA CHLE tests conducted in 2012 [1,2], as well as provide additional insight into the conditions that would cause precipitation and head loss during a LOCA at STP. Two 10-day tests were performed. These were designed to promote the generation of insoluble chemical products from corrosion sources; characterize any insoluble products that form with respect to product type, morphology, size, and formation location; evaluate the effect of zinc on the corrosion of aluminum; and evaluate the response of debris beds to the presence of supersaturated aluminum concentrations. Test T3 contained aluminum, zinc, galvanized steel, concrete, and fiberglass, whereas Test T4 contained only aluminum and fiberglass. The temperature was maintained at 80°C for 5 days to promote corrosion and then reduced to 35°C over the next 5 days to promote precipitation.

Role:	Name:	Signature:	Date:
Preparer:	Seung-Jun Kim	<signed electronically >	7/18/2013
UNM reviewer:	Kerry Howe	<signed electronically >	9/23/2013
UIUC reviewer:	Zahra Mohaghegh	<signed electronically >	8/3/2013 8/30/2013

Revision	Date	Description
0	7/18/2013	First draft
1	8/27/2013	Incorporates corrections from internal review
2	9/23/2013	Incorporates corrections from external review

Contents

List of Figures

List of Tables

1.0 Introduction

The Chemical Head Loss Experiment (CHLE) program was created to assess the chemical effects associated with resolution of generic safety issue (GSI) 191 at the South Texas Project (STP). The test series described in this report (Tests T3 and T4) evaluated chemical effects under conditions that promoted greater corrosion and chemical product release than expected under prototypical conditions at STP [3]. Prototypical chemistry conditions combined with an excess of aluminum material (having 100 times the surface-to-volume ratio found at STP) and a non-prototypical temperature profile were used for these tests. Tests T3 and T4 were intended to create conditions that promoted the generation of insoluble chemical products from corrosion sources with and without zinc source material (zinc coupons and galvanized steel coupons); characterize any insoluble products that form with respect to product type, size, and formation location; evaluate the corrosion of aluminum only; and investigate the response of debris beds (blender vs. NEI) to the presence of supersaturated aluminum concentrations.

Test T4 was designed to run for 10 days, but 2 days were added for a flow sweep test, making the test period May 10, 2013 to May 22, 2013. Test T3 ran for 10 days, from June 14, 2013 to June 24, 2013. These tests had the following characteristics, as described in more detail in reference [3]:

1. The non-prototypical temperature profile for Tests T3 and T4 was designed to promote the generation of chemical products from the corrosion material (aluminum, zinc, galvanized steel coupons).
2. Fiberglass volume was predicted by CASA, with 41% of test fiber used in the columns to produce fiber beds equivalent to past testing and the remaining quantity (59%) submerged in the corrosion tank.
3. Material was exposed to baseline chemicals of boric acid and lithium hydroxide from time zero, with incremental additions of tri-sodium phosphate (TSP), hydrochloric acid, and nitric acid.
4. Column approach velocity was 0.01 ft/s.
5. The 10-day testing involved two types of debris beds: blender-processed debris bed (columns 1 and 3) and NEI-processed debris bed (column 2).
6. Corrosion source materials used for tests T3 and T4 are listed in Table 1.

Table 1: Comparison of corrosion source material in T3 and T4

Corrosion source material	Test T3	Test T4
Al	30 ft^2 (submerged)	30 ft^2 (submerged)
Zn	126 ft^2 (submerged)	N/A
Galvanized steel	16 ft^2 (submerged)	N/A
Fiberglass	132.9 g (submerged)	132.9 g (submerged)
Concrete	0.81 ft^2 (submerged)	N/A

2.0 Process Monitoring

Process parameters required to perform the CHLE test were monitored continuously using a Compact-RIO acquisition system and the LabVIEW program. Tank temperature, pH, and velocity measurements

were continuously monitored and saved every minute to a spreadsheet for analysis. Results and discussion associated with these parameters are presented in the following sub-sections.

2.1 Tank temperature

The temperature profile for tests T3 and T4 was designed as shown in Figure 1, so that corrosion was promoted aggressively with a "worst (conservative) case scenario" of corrosion. In other testing (T1: Medium Break LOCA, T2: Large Break LOCA), the temperature profile during a test was as close to actual LOCA conditions as could be achieved with the current UNM testing apparatus. "Close to LOCA conditions" started with the tank at 85°C and then approximated the decreasing actual LOCA conditions, with segmented linear temperature profiles as close to the target as possible. Tests T3 and T4 started with the solution in the tank at 80°C, but instead of initiating the temperature profile control at time zero, the 80°C temperature was maintained for the first five days of the test. This temperature makes for a more corrosive environment than is typically present during a LOCA, based on predictions using the WCAP-16530-NP corrosion equation for aluminum. On day 5, the temperature began declining linearly, reaching 35°C on Day 10. The heaters in the tank maintain a "constant" temperature by cycling on and off. This causes a sinusoidal pattern in the tank temperature data, as can be seen in Figure 1.

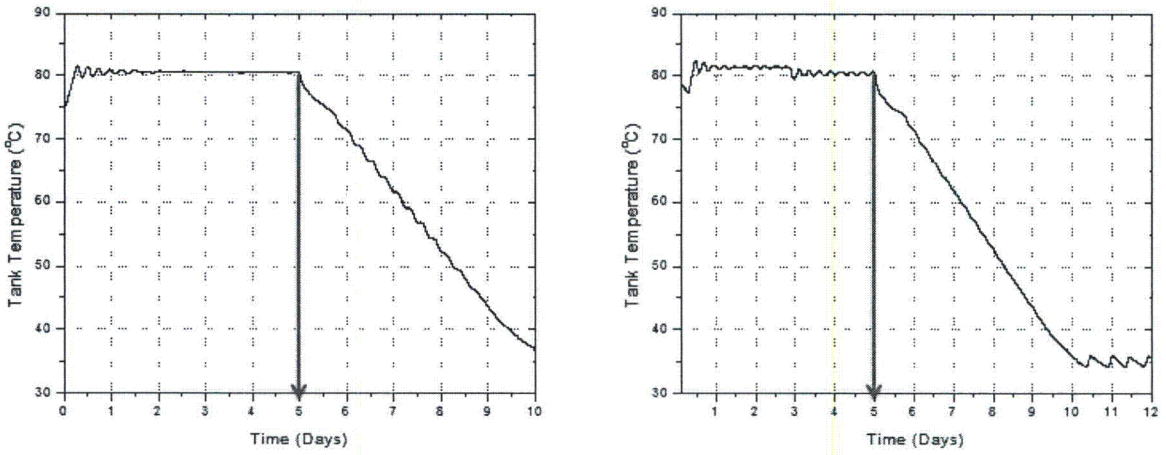

Figure 1: Experimental tank temperature profile for tests T3 (left) and T4 (right).

The tank temperature was slightly higher than the column temperature. This difference in temperature exceeded 1°C for the first four days and was less than 1°C for the remainder of the test. Therefore, the difference between the temperature of the solution in the tank and columns over the 10-day test was less than 1°C.

2.2 Solution pH

The solution pH was measured by both in-line and bench-top automatic temperature correction (ATC) pH meters. The on-line pH meter was calibrated using the pH 7 and the pH 10 standards. This two-point calibration might result in unreliable measurements below pH 7 for this test. Therefore the test solution pH was measured using the bench-top pH meter, which was calibrated using three pH values: 4.0, 7.0, and 10. The pH was measured twice per day. Above pH 7.0, the bench-top and on-line pH readings had a

0.1 pH unit margin of error. As determined by the bench-top pH meter, the solution pH at test initiation was 4.5 and increased to 7.3 during the addition of TSP. The solution pH measurement with bench-top ATC averaged 7.22 for the duration of both tests, as shown in Figure 2.

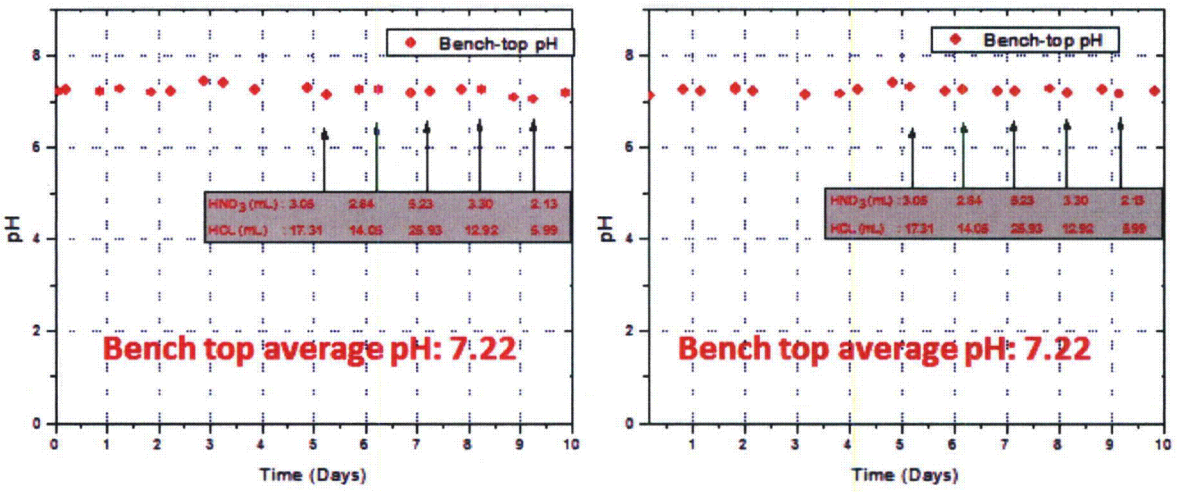

Figure 2: Test T3 (left) and T4 (right) test solution pH measurements with bench-top ATC.

2.3 Approach velocity

The approach velocity was maintained near 0.01 ft/s in all three columns throughout testing, as shown in Figure 3 for both Tests T3 and T4. The approach velocity for each column was adjusted by throttling a valve on the discharge side of the centrifugal pump, along with adjustment of the variable speed drive. The required approach velocity was below the minimum speed of the variable speed drive, which is why the variable speed drive and a valve were both necessary. Initial flow rate control was induced by throttling a valve on the discharge side of the pump and then finely adjusted using the variable speed drive. After completion of the 10-day tests, a flow sweep test was conducted by increasing the approach velocity to investigate the relationship between head loss and velocity in the blender-processed bed and NEI-processed bed. The flow sweep test results and discussion are included in Section 3.5.

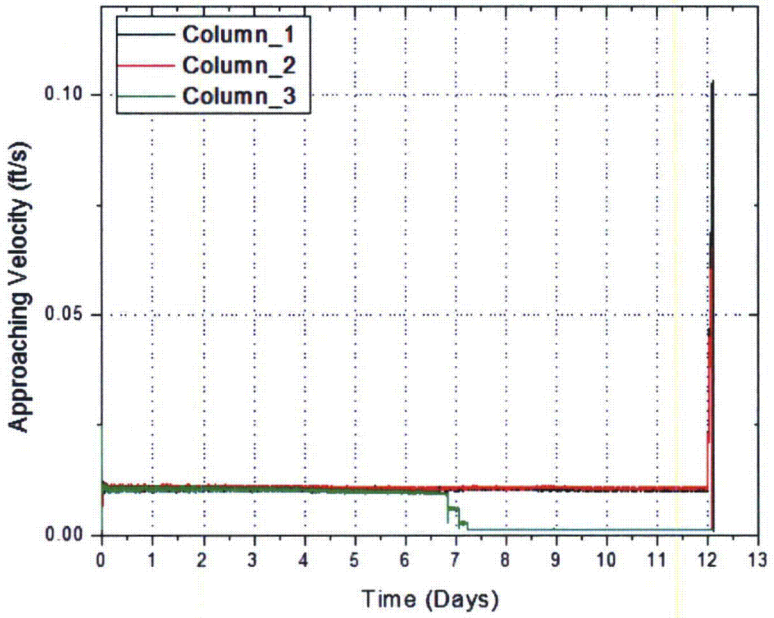

Figure 3: Approach velocity (0.01 ft/s) through fiberglass debris beds (Column 1, 2, and 3) for Test T4.

3.0 Results and Discussion

While process monitoring parameters were continually measured, some other parameters such as soluble metal concentration and turbidity were measured on discrete time frames. Samples for soluble metal concentration measurements were taken daily. Tank turbidity measurements were taken twice per day. Most importantly, the head losses for each column were monitored continuously for the 10-day testing period, with appropriate temperature correction. The results and discussion associated with these parameters are presented in the following sub-sections.

3.1 Solution chemistry and metal release

3.1.1 Turbidity trend with temperature profile

Turbidity measurements of the bulk test solution were collected daily at room temperature and at tank temperature. Three turbidity measurements of each sample were taken and averaged to ensure the accuracy of the measurement. In general, the discrepancy between the turbidity measurement at tank temperature and the turbidity measurement at room temperature were negligible in Tests T3 and T4, as shown in Figure 4(a). In the previous ICET tests, high concentrations of soluble aluminum (greater than 350 mg/L in ICET-1, which was conducted at high pH without TSP) were observed to precipitate rapidly when the solution was removed from the tank and began to cool. Rapid precipitation could interfere with turbidity measurements. The similarity between the turbidity measurements at tank temperature and room temperature in these tests indicates that precipitation did not occur rapidly when the solution

was removed from the tank, and therefore the turbidity measurements are a valid indication of the turbidity of the solution inside the tank.

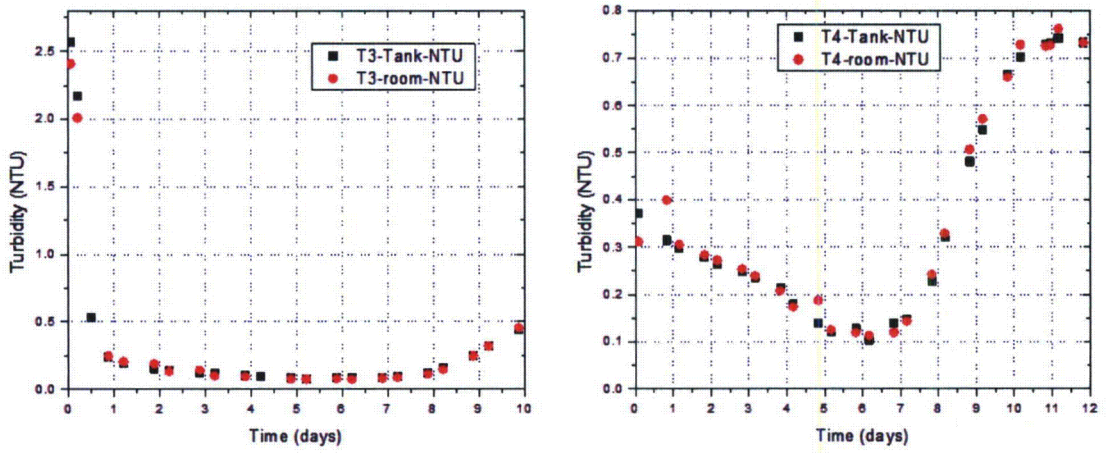

(a)

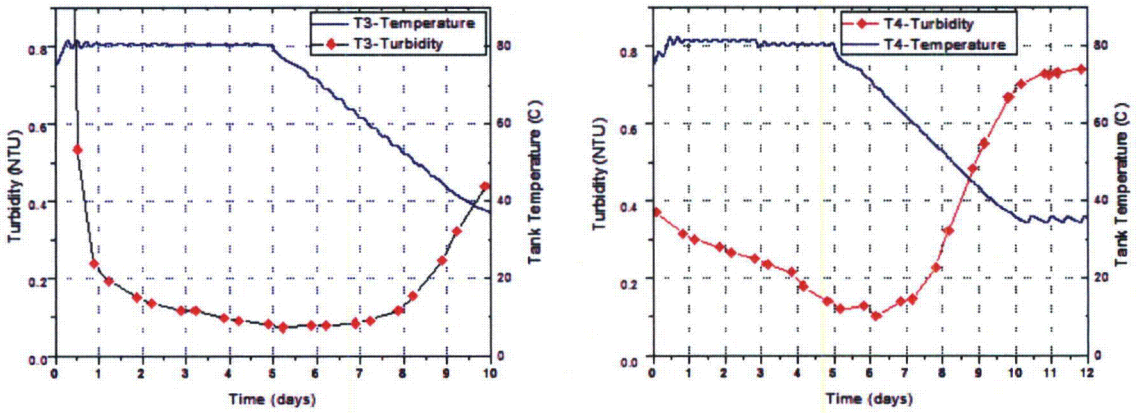

(b)

Figure 4: (a) Turbidity measurements at tank and room temperature for Tests T3 and T4, (b) correspondence between tank temperature and test solution turbidity measurements at tank temperature for Tests T3 and T4.

A turbidity increase indicates an increase in particles in solution. For Test T3, it was observed that the high turbidity reading (2.6 NTU) occurred 80 minutes into the test. At this time (t=80 minutes), all metal coupons had been in the tank since time zero, columns had been linked to the tank, and tri-sodium phosphate (TSP) had been added to the boric acid solution. By Day 1 (24 hours of operation), the turbidity decreased to 0.24 NTU and temperature was still high, at 80.3°C. This initial spike in turbidity appears to be related to the zinc, as discussed in the next section.

On Day 6, the temperature in Tests T3 and T4 decreased from approximately 80°C to approximately 72°C and continued to decrease. The turbidity reached a minimum on Day 6, with a low value of about 0.10 NTU in Tests T3 and T4. The turbidity increased from Day 7 to Day 10, reaching a high on Day 10 of 0.70 NTU in Test T4 and 0.50 NTU in Test T3. The increase in the turbidity shown in Figure 4(b) was

related to the decrease in temperature, which caused dissolved aluminum to start precipitating. The relationship between turbidity and metal concentrations is described in greater detail in the following section. Two extended days of testing were conducted in Test T4 to examine the turbidity behavior when the temperature was maintained at 35°C. The turbidity leveled off after 2 days at a constant temperature, suggesting that aluminum stopped precipitating when the temperature was constant.

3.1.2 Metal concentrations in solution

The total and filtered solution concentrations of aluminum, calcium, and silicon were measured daily during Tests T3 and T4 by inductively coupled plasma optical emission spectrometry (ICP-OES) analysis. Total concentration samples were immediately acidified for analysis; the filtered concentration samples were processed through a 0.10 μm filter before acidification to remove particles larger than 0.10 μm from solution. The filtered and total concentrations for the individual analytes taken from Days 1 to 10 were compared to determine whether the elements were in dissolved or particulate forms in the solution. Dissolved (soluble) forms of aluminum would not be captured by a filter. A difference in concentration between filtered and unfiltered (total) samples would indicate the presence of insoluble (solid) chemical product. The total and filtered aluminum concentrations are shown in Table 2 (for Test 3) and Table 3 (for Test 4). The differences between filtered and unfiltered (total) concentrations were insignificant, with average deviation of 0.086 mg/L or less. In some cases, the filtered sample had a higher concentration than the total sample, but the differences were typically 0.1 mg/L or less, which is the limit of sensitivity of the analytical instrument. During the time these tests were conducted, the relative standard deviation (RSD) of the analytical method was 4.8%, thus, the variation between total and filtered results is due to normal variability in the measurements. Variability becomes particularly important when the filtered and total sample concentrations are identical, in which case one measured concentration can be slightly above the other. The variability can appear more significant when the results are near the detection limit or below the laboratory's standard reporting limit. For this reason, the filtered and unfiltered (total) concentrations are considered identical, and it is assumed that there is no evidence of the presence of larger than 0.10 μm insoluble (solid) chemical product in the solution. In this group of tests, the calcium concentration was below the laboratory's reporting limit of 10 mg/L.

Table 2: Test T3 comparison of filtered and unfiltered measured concentrations

Day	Al total (mg/L)	Al filtered (mg/L)	Absolute deviation (mg/L)
0.06	< 0.2	< 0.2	0.00
1	2.2	2.2	0.00
2	2.5	2.5	0.00
3	2.5	2.5	0.00
4	2.4	2.5	0.10
5	2.8	2.7	0.10
6	2.7	2.7	0.00
7	2.4	2.4	0.00
8	2.1	2.0	0.10
9	1.8	1.7	0.10
10	1.6	1.6	0.00

Table 3: Test T4 comparison of filtered and unfiltered measured concentration

Day	Al total (mg/L)	Al filtered (mg/L)	Absolute deviation (mg/L)
0	0.20	0.32	0.12
1	4.0	4.0	0.00
2	5.1	5.1	0.00
3	5.0	5.1	0.10
4	4.9	4.9	0.00
5	4.9	5.0	0.10
6	4.8	4.5	0.30
7	3.8	4.0	0.20
8	3.2	3.1	0.10
9	2.6	2.6	0.00
10	2.6	2.5	0.10
11	2.6	2.5	0.10
12	2.6	2.6	0.00

The aluminum concentration increased during the first two days, reaching 2.5 mg/L in Test T3 and 5.1 mg/L in Test T4 on Day 2, as shown in Figure 5(a). From Day 3 through Day 5, when the temperature was held constant, the concentration for Test T3 and T4 stayed approximately constant until Day 5: Test T3 increased slightly to 2.7 mg/L, whereas that for Test T4 decreased slightly to 5.0 mg/L. These slight variations may be due to the variability in the measurements, since the differences are near the resolution of the instrument (0.1 mg/L) and within the RSD mentioned earlier . The concentration declined during Days 5 to 10, during which the temperature in the tank was declining. The reduction in the total aluminum concentration indicates that some precipitates have been removed from solution by filtration as shown in Figure 5(b). The final measured aluminum concentration was 2.6 mg/L in Test T4 and was the same on Days 9 and 12, indicating that the aluminum concentration became constant when the temperature became constant.

Aluminum readily forms an oxide layer when exposed to the atmosphere [7]. At high temperatures and low pH, this aluminum oxide layer dissolves in solution, at which point the aluminum coupon can corrode. In a neutral solution, a passivation layer such as aluminum phosphate can form and corrosion will slow down or cease altogether. In the first two days of Tests T3 and T4, corresponding to the highest temperature of the test period, aluminum concentration increased from zero to its maximum.

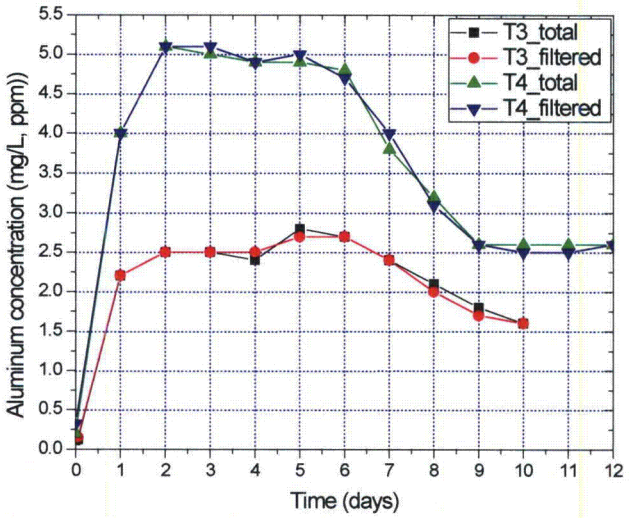

(a)

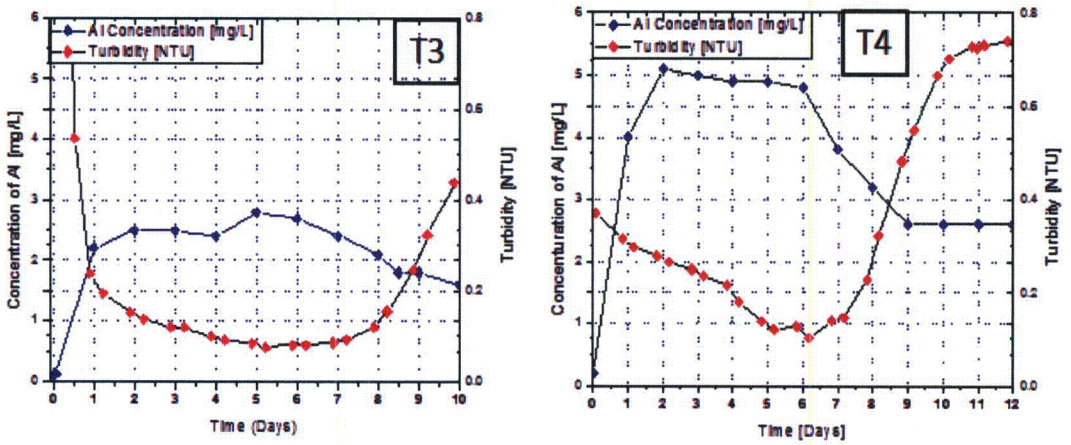

(b)

Figure 5: (a) measured aluminum concentration in Tests T3 and T4 and (b) Al concentration with turbidity trend Tests T3 and T4.

Calcium and silicon are leached products of fiberglass. In Test T4, calcium and silicon measured at their lowest (0.95 and 4.1 mg/L, respectively) at time zero and increased steadily to about Day 6, reaching their highest concentration (2.1 and 15 mg/L, respectively). After Day 6, calcium concentration fluctuated slightly, decreasing to as low as 1.5 mg/L, and silicon concentration remained fairly steady, as shown in Figure 6(a). In Test T3, silicon again had its lowest concentration (4.3 mg/L) at time zero and highest concentration (13 mg/L) around Day 6. Calcium, on the other hand, reached its highest concentration at 80 minutes and then fluctuated between 0.72 and 1.4 mg/L for the remainder of the test, as shown in Figure 6(a). The reason for the lower concentrations of Ca and Si in Test T3 than in Test T4 has not been identified, but it may be due to interaction with zinc.

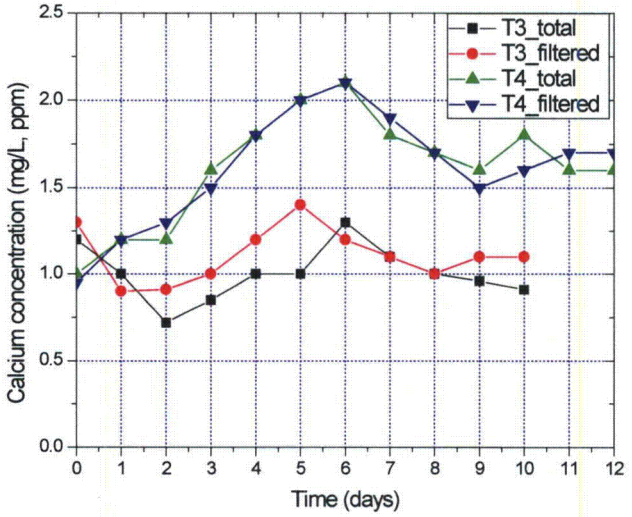

(a)

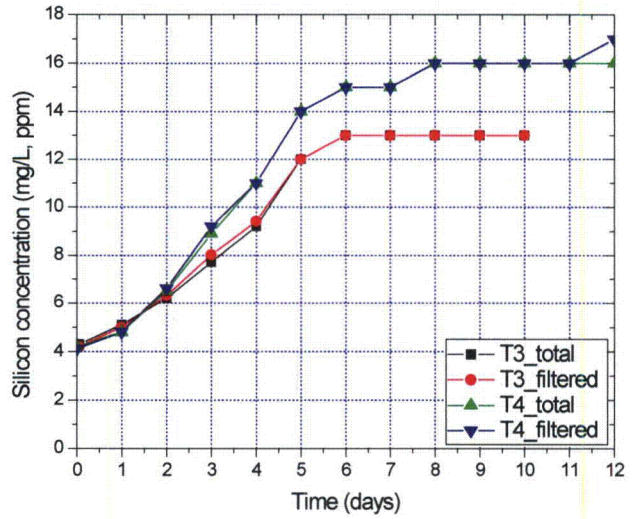

(b)

Figure 6: Measured calcium (a) and silicon (b) concentration in Tests T3 and T4 and silicon concentration.

Zinc coupons were included in the Test T3, with its highest total concentration (1.5 mg/L) and highest filtered concentration (0.44 mg/L) occurring at 80 minutes (Table 4). The difference indicates more than 0.10 µm of particulate in solution. The analysis for Test T3 indicated that the particle size at 80 minutes was about 1.9 µm, and then the size decreased with time. The detailed analysis for particle size will be presented in the following section. The measured concentration of zinc (total and filtered) decreased to approximately 0.30 mg/L on Day 2 and continued to decrease, reaching a minimum concentration of 0.095 mg/L on Day 8. The zinc particles in solution affected the turbidity. Test T3 showed initial high

turbidity (2.6 NTU), as shown in Figure 4(a), where the zinc has highest concentration. This peak in turbidity was brief and followed by rapid decline, falling below 0.5 NTU by the end of the Day 1. In contrast, Test T4 turbidity stayed below 0.5 NTU for Day 1 through Day 8. The decrease in turbidity is consistent with the decrease in particulate zinc shown in Figure 7, and the larger size of the particles explains their more rapid removal from the tank. Similar behavior was not seen in Test T4, and Test T4 had no zinc or galvanized steel present during testing.

Table 4: Test T3 comparison of filtered and unfiltered measured concentrations of zinc

Day	Zn total (mg/L)	Zn filtered (mg/L)	Absolute deviation (mg/L)
0.06	1.5	0.44	1.06
1	0.29	0.25	0.04
2	0.30	0.30	0.00
3	0.27	0.25	0.02
4	0.23	0.21	0.02
5	0.21	0.19	0.02
6	0.18	0.18	0.00
7	0.13	0.13	0.00
8	0.10	0.095	0.01
9	0.12	0.11	0.01
10	0.16	0.15	0.01

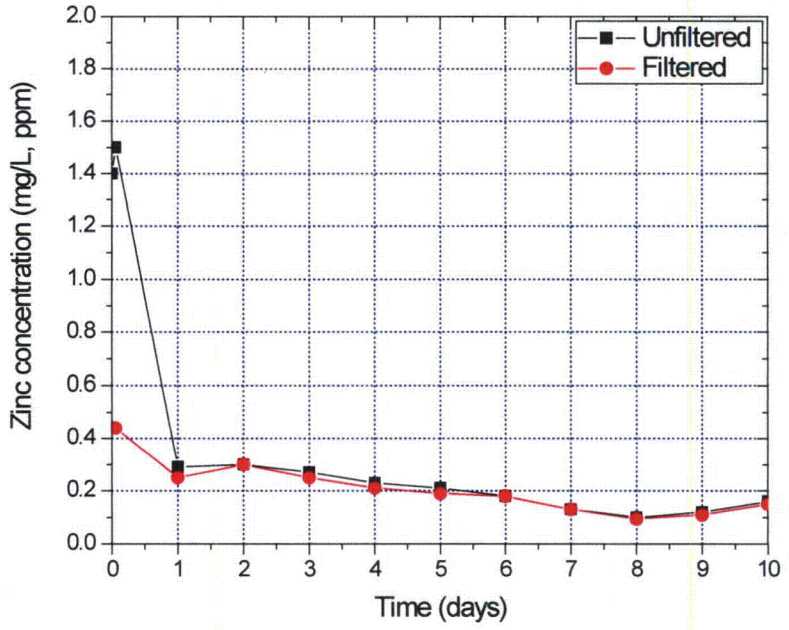

Figure 7: Test T3 measured zinc concentration over time (unfiltered and filtered)

In these tests, the measured aluminum release rates were substantially lower than the corresponding release rate determined from WCAP-16530-NP [4]. After day 2, measured aluminum concentration for

Test T3 reached 2.5 to 2.7 mg/L; while Test T4 measured aluminum concentration was as high as 5.1 mg/L. The WCAP prediction for aluminum concentration was determined from the temperature, pH, and accumulated aluminum release as of each day, and was compared with measured aluminum concentration from ICP-OES. The predicted WCAP concentration was more than 4 times higher at Day 1 and continued to increase. The results shown in Figure 8 indicated that the WCAP-16530-NP equation significantly overestimated the aluminum concentration, possibly because it does not account for passivation or corrosion-inhibiting effects.

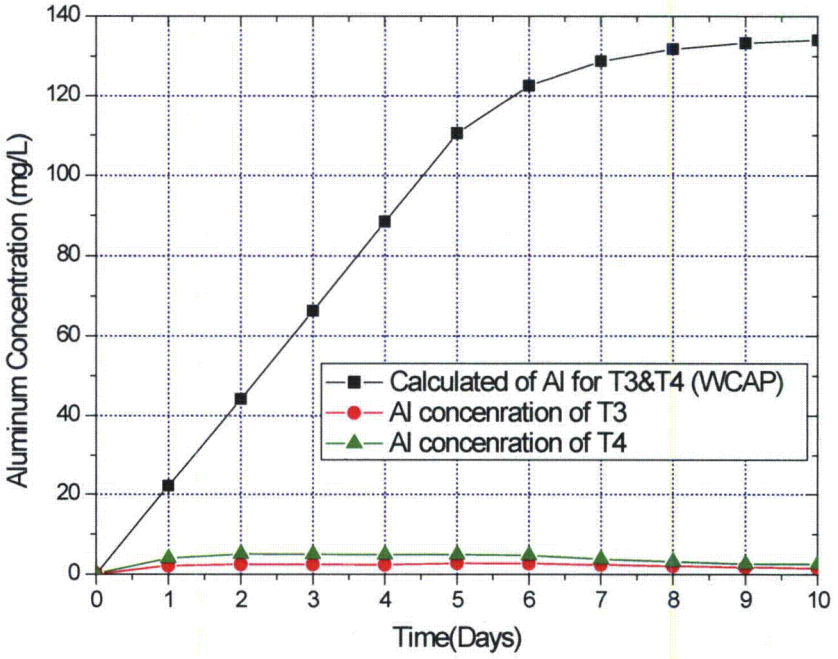

Figure 8: Test T3 and Test T4 measured release compared to WCAP predicted release.

3.1.3 Aluminum Hydroxide precipitation map based on Visual MINTEQ

A comparison of measured aluminum concentration in solution to the saturation concentration (solubility) in equilibrium with aluminum hydroxide demonstrates that the aluminum concentrations measured in solution during the first five days were not limited by the saturation concentration limits, as shown in Figure 9. Also, the measured aluminum concentration does approach the saturation concentration after day 5 because the saturation concentration rapidly declines as temperature decreases. Although Figure 9 indicates that the concentration of aluminum in these tests does not exceed the solubility limit of $Al(OH)_3$ until Day 9, some variability in the temperature dependence of aluminum saturation occurred due to competing reactions among the many constituents in solution. The relationship between the concentration in these tests and the $Al(OH)_3$ solubility limit is explored in the context of other literature below.

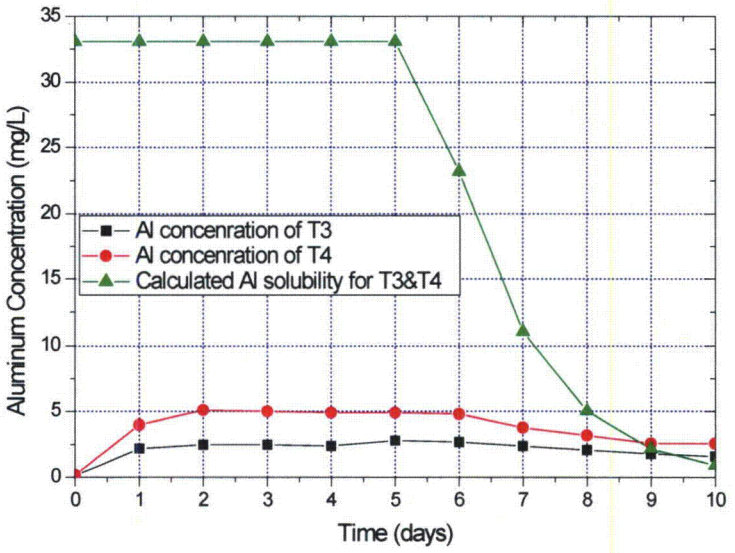

Figure 9: Test T3 and Test T4 concentration in solution and solubility curve for aluminum hydroxide $Al(OH)_3$. Solubility of $Al(OH)_3$ is calculated at pH=7.2 using Visual MINTEQ.

Bahn et al. (2011) developed an aluminum hydroxide precipitation map in the "pH + $p[Al]_t$" vs. temperature domain based on ANL's Bench test top, ANL's loop test data, and other literature data [5]. Since using pH + $p[Al]_t$ is a convenient way to display and compare solubility test results obtained under various test conditions, UNM's Test T3 and Test T4 results were incorporated into Bahn's aluminum hydroxide precipitation map to generate the precipitation window for Tests T3 and T4. The boundary of precipitation region and non-precipitation region corresponded roughly to the solubility of $Al(OH)_3$ determined by Visual MINTEQ, highlighted in blue in Figure 10(a). The precipitation window was defined with a ±8°C temperature range at the fixed pH condition (7.22 for Tests T3 and T4) and the highest (which is the most conservative value) Al concentration over the 10-day test (2.5 mg/g at day 2 in Test T3 and 5.1 mg/L at day 2 in Test T4). The precipitation windows for Tests T3 and T4 were determined as encompassing the temperature ranges of 44°C to 60°C, and 47°C to 63°C, respectively. Incorporating the Al precipitation window with UNM's Test T3 and Test T4 temperature and turbidity data indicates that Al precipitation would take place around day 7 to day 9 in both tests, where the turbidity started increasing notably, as shown in Figure 10(b). The comparison between the concentration of aluminum in Tests T3 and T4 with the $Al(OH)_3$ precipitation map developed by Bahn et al. demonstrates that precipitation occurred approximately when it should have (Day 6 or 7) for the given temperature, pH, and [Al] conditions of the test. This analysis demonstrates that the expected behavior was consistent with the turbidity and aluminum concentration data. In addition, the "pH + $p[At]_t$" values from CHLE Tests T1 and T2 are also shown on Figure 10(a). For those tests, the pH + $p[At]_t$ values stay within the soluble region for the entire duration of the tests. Thus, this analysis validates the turbidity and aluminum concentration data collected in Tests T1 and T2, which indicated that precipitation did not occur.

(a)

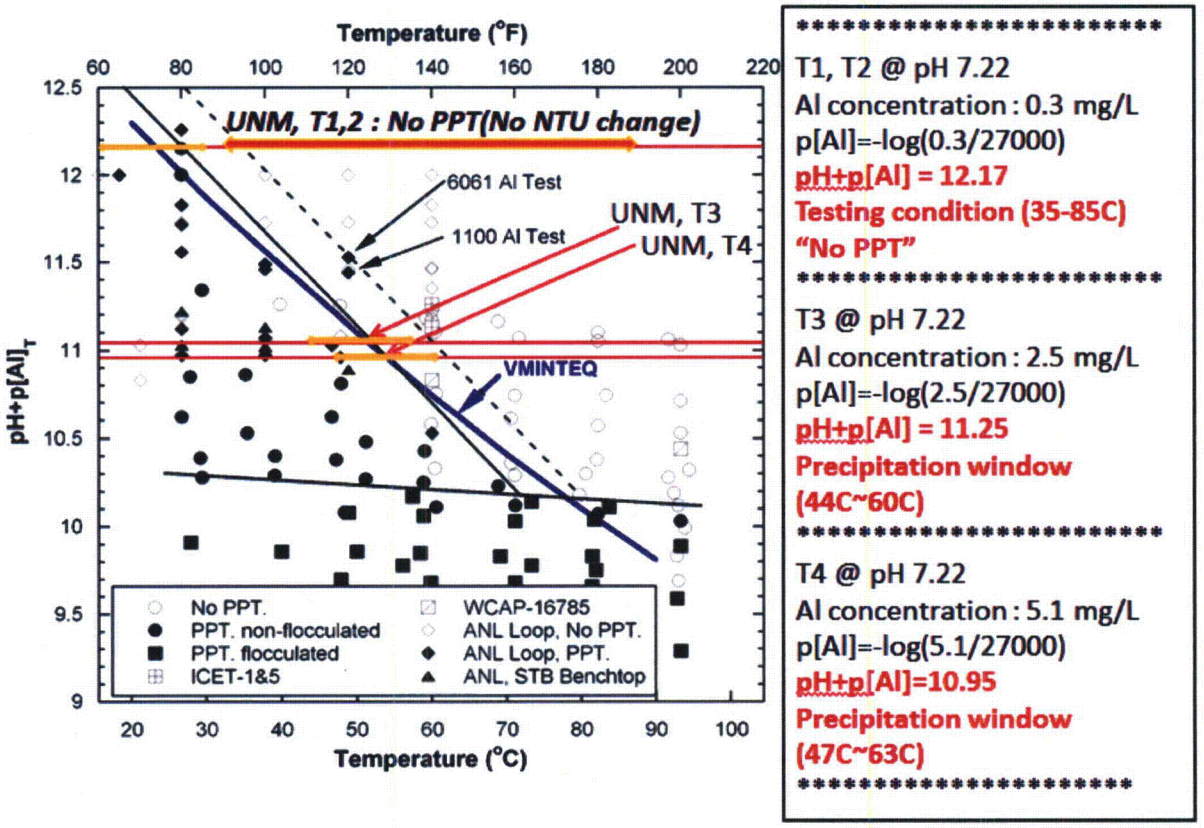

(b)

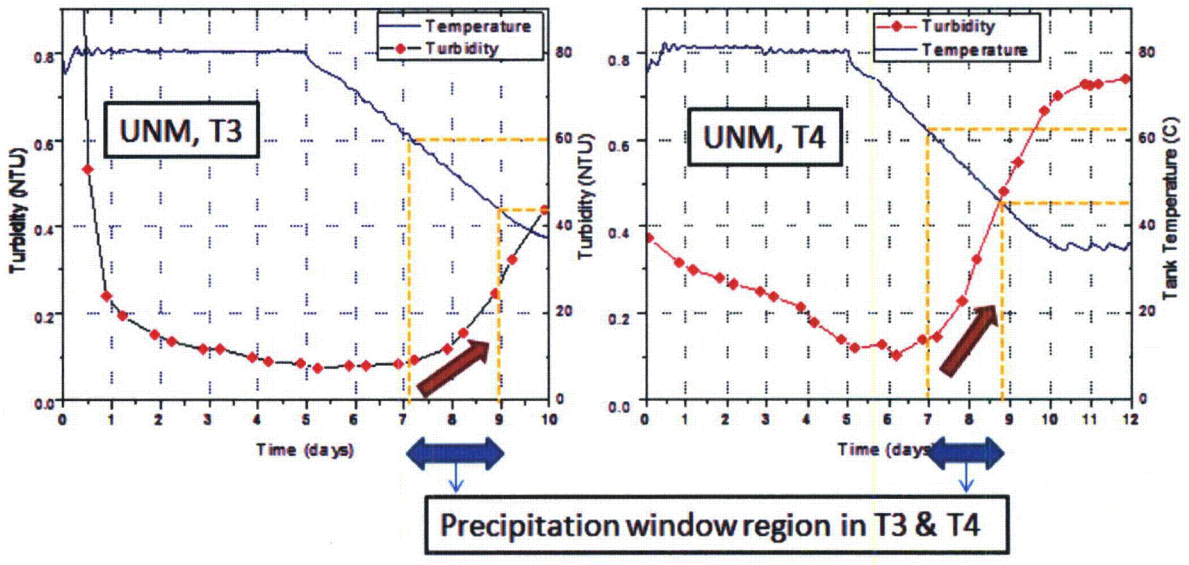

Figure 10: (a) Al precipitation window for UNM Tests T3 and T4 based on Bahn's (2011) aluminum hydroxide precipitation map, (b) corresponding turbidity data for Tests T3 and T4 with precipitation windows.

3.1.4 Zeta potential and particle size analysis

Samples of test solution for Tests T3 and T4 were taken in a clear disposable zeta cell to measure zeta potential and particle size. Both particle size and zeta potential measurement were carried out using the Zetasizer Nano ZS (Malvern-ZPS). For each sample, measurements were carried out at least in triplicate. Attempts were made to determine suspended particle size distribution using dynamic light scattering (DLS) and to measure zeta potential by using laser Doppler micro-electrophoresis.

Zeta potential may play a role in the CHLE experiments with a respect of suspended corrosion production and possible precipitate occurrence in the test, because it governs the stability of particles suspended in the test solution. If the zeta potential is strongly negative, particles tend to stay suspended due to its repulsive force. If the zeta potential is close to neutral, the particles can group together and possibly flocculate. Zeta potential was averaged from six runs at 25°C. The Zetasizer Nano ZS calculates the electrophoretic mobility of the particle and converts it to zeta potential using the Smoluchowski equation. Zeta potential measurement indicates the overall surface charge of the particles in a given environment. Zeta potential is affected by changes in the environment (e.g., pH). The zeta potential values for Tests T3 and T4 ranged from -25 mV to -35 mv over the 10-day as shown in Figure 11(a).

Particle size measurement gives the radius of a sphere having the same volume as the particle. Dynamic light scattering is a way to measure particle size using intensity fluctuations in scattered light that is provided by a laser. These fluctuations are caused by the Brownian motion of the suspended particles in the solution. Brownian motion is directly related to particle size. The light scattering of smaller particles will fluctuate faster than that of larger ones. The size can then be calculated from the Stokes-Einstein equation. In both Test T3 and Test T4, particle size and turbidity had a positive correlation.

During the first 2 days of testing, the particles were larger than later in the test. At day 0 (t=80 minutes), Test T3 had large particles, averaging 1900 nm, while T4 had smaller particles, averaging 350 nm. These large particles eventually filter out of solution via the debris beds over the rest of the Tests T3 and T4, as seen in Figure 11(b). By the Day 2, the particles in Test T3 are below 200 nm. The turbidity for Test T3 follows a similar trend, with high turbidity on day 0 and having a rapid drop by day 1. Test T4 has small particles and low turbidity throughout the 10-day testing.

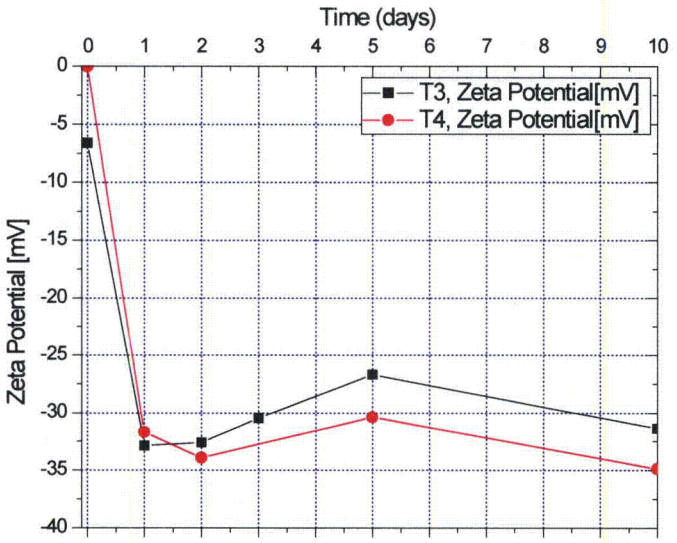

(a)

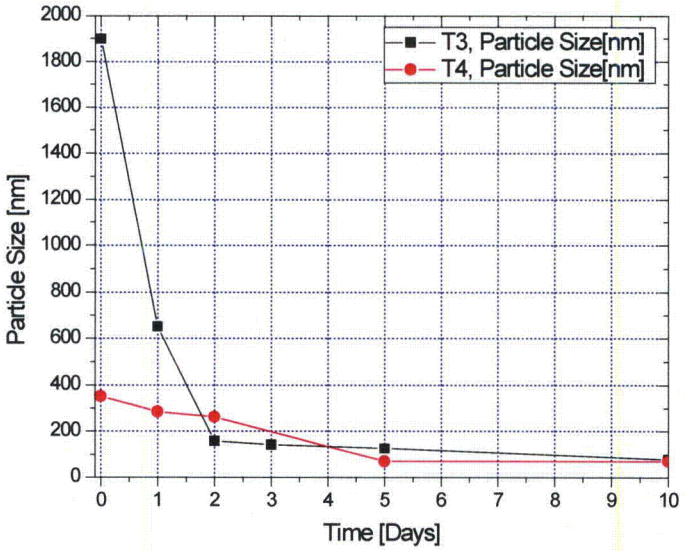

(b)

Figure 11: Selected day samples in Tests T3 and T4 of (a) Zeta potential and (b) particle size.

The main differences between Tests T3 and T4 was the presence of zinc in the Test T3 solution (from galvanized and pure zinc coupons) and the large particle size at the beginning of Test T3. Thus, the large particles were likely introduced into solution from the zinc itself, which could be called the zinc source effect. This release was not a result of corrosion during the test and appears to be particles being "washed" off the zinc by the high temperature environment during the first hour of testing.

3.2 Bed examination

After Tests T3 and T4 were complete, the fiber beds were removed from the columns for post-test analysis. During testing, the debris beds in Column 3 in Test T4 and columns 1 and 3 in Test T3 reached a head loss that was deemed too high for safe operation. Subsequently, Column 3 in T4 and column 1 and 3 in Test T3 were stopped at day 7 and day 8, respectively, and were isolated from the tank system for the rest of the testing period.

Two types of fiberglass beds were used during Tests T3 and T4. Columns 1 and 3 in Tests T3 and T4 were loaded with blender-processed debris beds, and Column 2 in Tests T3 and T4 was loaded with the NEI-processed debris bed. By the end of Test T3, the blender-processed debris beds exhibited approximately 150'' of H_2O normalized head loss for columns 1 and 3, and the NEI-processed debris bed indicated around 0.5'' of H_2O normalized lead loss. In Test T4, the blender-processed debris beds exhibited much higher normalized head loss maximums of 13" and 150" of H_2O for columns 1 and 3, respectively, than the NEI-processed debris bed, column 2, which had a maximum normalized head loss of around 0.5" of H_2O.

Following the extraction of the beds from each column at the end of test, a visual analysis of the fiberglass beds was performed for Tests T3 and T4. Figure 12 showed the post blender-processed debris beds with bottom of each bed was being removed and peeled back.

Figure 12: Blender-processed beds in Column 1 after exposure to 10-day test in Test T3 (left) and Test T4 (right).

Visual inspection showed that there were very few particles on the surface of the beds, besides the small white particles found in previous tests. The sparse white particles on the surface of the beds in previous tests sometimes appeared even before the CHLE tank was linked to the columns without causing any head loss.

Figure 13: NEI-processed beds in Column 2 after exposure to 10-day test in Test T3 (left) and Test T4 (right).

Figure 13 showed the post NEI-processed debris beds in Column 2 after extraction from the test. These beds did not show significant signs of fiber penetration into the pores of the screen, possibly because the characteristic length of the fiber used is much longer than that of the blender-processed fiber. The local porosity of the fiberglass inside the pores of the screen is believed to be the primary cause of head loss.

Figure 14 Blender-processed beds in Column 3 after exposure to 10-day test in Test T3 (left) and Test T4 (right).

The last visual observation was the visible dark spots on the bottom of Column 3 in Tests T3 and T4, as shown in Figure 14. These dark spots, or dimples, appeared on the bottom layer of fiberglass in Columns 1 and 3. These dimples were in response to the fibers filling the holes in the support screen. The dimples were more prominent in Column 3 than Column 1. The dark dimples shown in Figure 14 (right) were not found in the other two beds in Test T4. There is no definitive explanation as to why Column 3 in Test T4 would have dark spots and that test's other two columns would not. The dark spots appear to be particulate matter that migrated to the bottom of the debris bed and clogged the pores of the fiber bed at the screen pore sites. This increased clogging could explain why Column 3 in Test T4 experienced higher head loss than the bed in Column 1 in Test T4.

Figure 15: Close look on dark dimple found in blender-processed fiber beds in Tests T3 and T4 (left), chunk of fiberglass from the mesh bag after exposure to 10-day test solution (right).

Figure 15 showed a comparison of the blender beds to that of the fiberglass found in the CHLE tank. The beds appear to have lost their original colors as compared with the fiberglass bag from the tank. There was also no visible difference between pre-test and post-test fiber in the fiberglass bag from the CHLE tank.

3.3 Normalized head loss

Normalized head loss is measured in the CHLE testing series [3]. Tests T3 and T4 used the two types of beds simultaneously during the 10-day test period. The two beds in columns 1 and 3 were the blender-processed debris beds, which are thought to be highly sensitive in terms of head loss change, but less reproducible and not as likely to form under actual LOCA conditions. Column 2 contained an NEI-processed debris bed, which is less sensitive, but more reproducible and believed to be more representative of the type of debris that would be found during a LOCA. These beds may serve as a nucleation site for or a filter of possible chemical products that may form during the 10-day test. The two debris beds are shown in Figure 16.

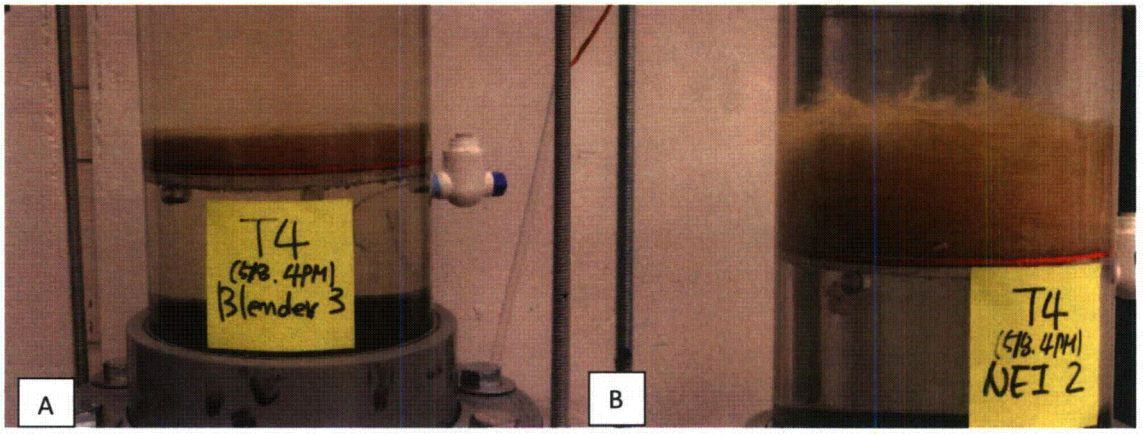

Figure 16: Blender-processed (a) and NEI-processed (b) debris beds used in this test.

Due to the non-isothermal condition between testing apparatus (columns) and measurement device, the head loss measurement needed to be normalized to a reference temperature, which in Tests T3 and T4 was 20°C. Change in temperature will affect density and viscosity, which in turn affect the overall head loss. The maximum head loss discrepancy due to normalizing density as a function of temperature is small, about 0.75 inches of water at the temperatures used in this study. However, the temperature effects on viscosity have a significant impact on normalizing head loss. Normalizing to the reference temperature for both viscosity and density is done using the equation listed below:

$$H_{L,c} = (DP_{raw} + (\rho_t - \rho_{rt})gh)(\frac{\mu_{std}}{\mu_t}) \quad (1)$$

where,

- $H_{l,c}$ is the normalized head loss
- DP_{raw} is the instrument differential pressure measurement
- ρ_t and ρ_{rt} are the densities at test temperature(t) and at room temperature (rt)
- g is the gravitational constant
- h is the vertical height between the upper DP sample tap and the DP cell
- μ_t and μ_{std} are the viscosity at test temperature(t) and at standard temperature (std) of 20°C

The temperature in the upper leg of the DP cell is not measured but estimated to be equivalent to room temperature.

The normalized head loss was significantly different among the three columns in Test T4. The rate of normalized head loss increase in Column 1 was much higher than that in column 2, as shown in Figure 17. This shows how much more sensitive a blender-prepared debris bed (column 1) is than an NEI-prepared debris bed (column 2). Column 3's blender bed was so sensitive that the normalized head loss in the first five days of testing prompted the shutdown of column 3 so as not to damage equipment.

The responses of the two types of debris beds were very different. The NEI-processed debris bed is more representative of the debris that is expected to form during a LOCA, and the head loss through the NEI-processed debris bed was not as responsive as a blender bed is to the presence of materials circulating with the water. The head loss in column 2 (NEI bed) during Test T4 increased from about 0.1 inches of water at time zero, to around 0.5 inches of water at the end of 10-day testing. Comparing the head loss in the NEI-processed debris bed to that in the blender-processed debris beds, demonstrates the sensitivity of the blender-processed debris beds. While the NEI-processed debris bed had a head loss increase of only about 0.5 inches over the 10 days, as shown in Figure 17, the blender bed in column 1 increased almost 12 inches in the same amount of time. The blender bed in column 3 was more sensitve than the column 1 bed. In just seven days, Column 3 head loss increased over 140 inches of water, as also shown in Figure 18.

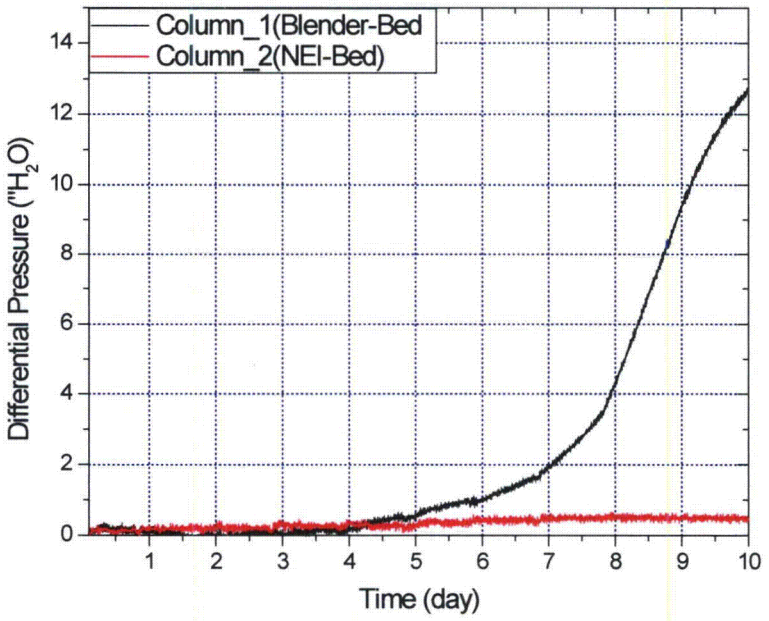

Figure 17: Normalized head loss through NEI-processed fiberglass debris bed for Test T4.

The rapid decrease in turbidity and particulate zinc in Test T3 corresponds to an increase in head loss in all three columns. Columns 1 and 3 increased to over 100 inches of normalized head loss within the first day, and Column 2 doubled from 0.3 inches to more than 0.6 inches in the same period, as shown in Figure 18. These results indicate that both blender-processed and NEI-processed debris beds capturing particles and caused normalized head lose increase, but the blender-processed beds are much more sensitive to the presence of particles. It also shows that as these particles were being captured, the beds were filtering them out of solution, and as a result the turbidity decreased.

The blender-processed beds had two distinctive periods of increasing head loss. In Test T3, the first period of increasing head loss due to the filtration of particulate zinc started on Day 1, and a second period of increasing head loss happened after approximately Day 6. This increase in normalized head loss was at approximately the time (Day 6 or 7) that the aluminum concentration started decreasing and the turbidity started increasing, so the increase appears to be related to the precipitation of aluminum. In Test T4, the head loss in Column 1 started increasing gradually around Day 4 and the head loss in Column 3 started increasing rapidly around Day 3.5. In Column 3, the normalized head loss rose to about 80 inches and started gradually decreasing due to the restructuring of the beds, suggesting that the conditions that had caused the head loss were disappearing. At Day 6, the head loss again started increasing rapidly in Column 3, and a day later the head loss in Column 1 also started increasing rapidly. The increase in head loss starting on Day 6 or 7 appears to be related to the precipitation of aluminum, since the head loss corresponds to about the time when the aluminum concentration was decreasing and the turbidity was increasing. As was shown in particle size analysis and precipitation window

analysis based on the Visual MINTEQ in Section 3.1, the particle sizes of zinc at Day 0 in T3 were larger than 1 µm, which could have been responsible for the initial rapid head loss increase in Test T3. The aluminum precipitation during Days 7-9 in Tests T3 and T4 could have accounted for another head loss increase. However, the increase in head loss from Day 3.5 to Day 6 is more difficult to explain. The aluminum concentration data show that a slight decrease of 0.1 mg/L may have occurred on Day 4 or 5, but the resolution of the ICP-OES measurements are only to the nearest 0.1 mg/L and the RSD of the instrument was 4.8%, so the variation in concentration was within the normal variability of the test method and cannot be interpreted as a decrease in aluminum concentration. In addition, the removal of aluminum increased over the next several days, but the head loss in Column 3 started to level off, which is not consistent with continued precipitation.

T3

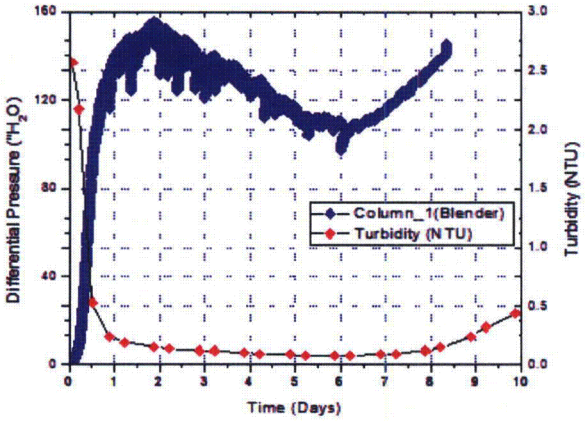

T4

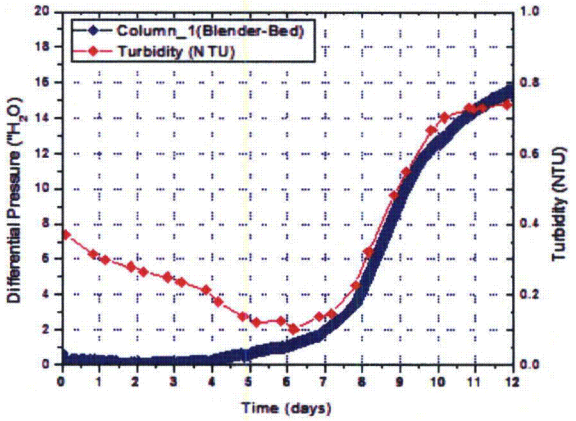

T3

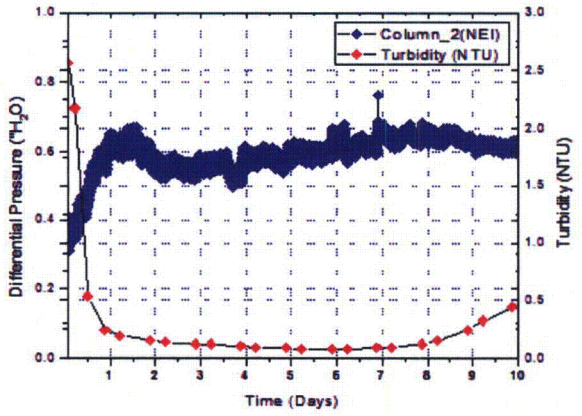

T4

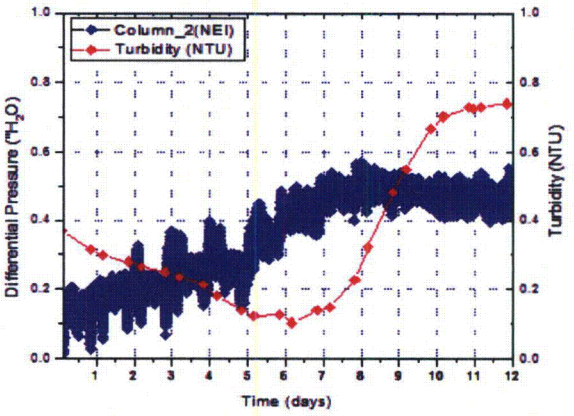

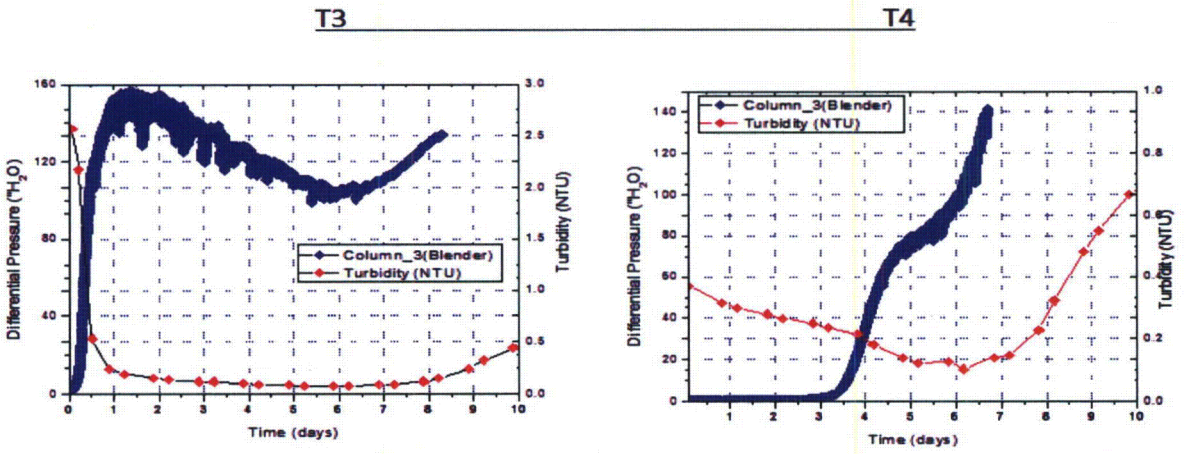

Figure 18: Normalized head loss measurements produced by all three columns for Tests T3 and T4.

Test T3 experienced two periods of increasing normalized head loss, while Test T4 had increasing head loss only in the latter part of the test. The rapid head loss increasing after loading during Test T3 can be attributed to the addition of zinc to the tank and has been named the "Zn source effect." The head loss occurring later in the experiment could be attributed to the "Al precipitate effect," and the turbidity was observed to increase in Tests T4 and T3 past Day 7. These two effects can be seen graphically in Figure 19. However, the increasing normalized head loss from Days 3.5 to Day 6 in Test T4 cannot be explained by either of these phenomena and may be due to the continued filtration of latent debris in the tank solution.

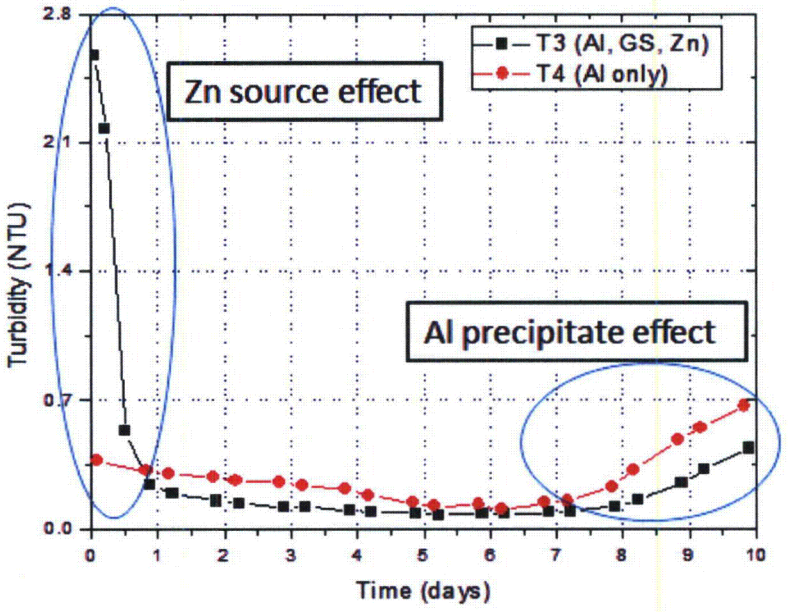

Figure 19: Zn source effect and Al precipitate effect on head loss increase.

3.4 Corrosion (weight loss, XRD, SEM-EDX, and XPS)

Aluminum corrosion is the sum of the aluminum mass released into solution and the mass assimilated into the scale layer on the corroded material itself, as defined by Equation 2. Once in solution, the corroded aluminum can remain in solution, precipitate and be separated from solution by sedimentation or filtration, or form scale on other surfaces in the system, as shown by Equation 3. The concentration of material remaining in solution is measured by inductively coupled plasma optical emission spectrometry (ICP-OES). The mass balance requires the mass of corroded aluminum incorporated into the scale.

$$Al_{corroded} = Al_{scale} + Al_{released} \quad (2)$$

$$Al_{released} = Al_{soluble} + Al_{precipitated/scale} \quad (3)$$

To determine the mass of corroded aluminum that was incorporated into the scale layer on the material itself requires the knowledge of the original and final scale composition.

3.4.1 Weight loss

In Test T4, aluminum coupons were the only source of aluminum. The mass change was measured, but showed very little change, with an average mass loss of 0.037 g per coupon. The only major change was in the surficial color of the aluminum: from light grey to dark grey. In contrast to Test T4, Test T3 found that aluminum, zinc, and galvanized steel coupons were the main sources of corrosion. The mass change was measured for all individual coupons. The aluminum coupon mass change in Test T3 was mass gain instead of mass loss, averaging 0.042 g, as shown in Table 5. The average mass gains for zinc and galvanized steel in Test T3 were 0.451 g and 0.318 g, respectively. The mass loss in Test T4 suggests Al corrosion and release into the solution, and the mass gain in Test T3 demonstrates that the corrosion products were deposited into the all of the coupons. The zinc phosphate compound deposition in all coupons in Test T3 will be presented in following section (SEM-EDS analysis).

Table 5: Aluminum coupon masses before and after the 10-day test for Tests T3 and T4

Aluminum coupon mass loss in Test T3 (average Al mass gain: 0.042 g)					
Metal	**Coupon #**	***Rack Position***	**Pre-Test Mass (g)**	**Post-Test Mass (g)**	**Mass Loss(g)**
Aluminum	A001	*A-11*	397.96	397.99	-0.03
Aluminum	A002	*A-13*	397.40	397.44	-0.04
Aluminum	A003	*A-22*	399.26	399.32	-0.06
Aluminum	A004	*A-23*	397.77	397.81	-0.04
Aluminum	A005	*A-24*	397.43	397.48	-0.05
Aluminum	A006	*A-25*	399.15	399.19	-0.04
Aluminum	A007	*A-26*	399.16	399.21	-0.05
Aluminum	A008	*A-27*	400.56	400.62	-0.06
Aluminum	A009	*B-22*	398.50	398.59	-0.09
Aluminum	A010	*B-23*	398.85	398.85	0.00
Aluminum	A011	*B-24*	397.45	397.50	-0.05

Aluminum	A012	*B-25*	400.11	400.14	-0.03
Aluminum	A013	*B-26*	398.68	398.72	-0.04
Aluminum	A014	*B-27*	400.66	400.70	-0.04
Aluminum	A015	*B-37*	399.69	399.71	-0.02
Aluminum coupon mass loss in Test T4 (average Al mass loss: 0.037 g)					
Metal	**Coupon #**	***Rack Position***	**Pre-Test Mass (g)**	**Post-Test Mass (g)**	**Mass Loss (g)**
Aluminum	A001	*2*	396.82	396.73	0.09
Aluminum	A002	*7*	399.09	399.03	0.06
Aluminum	A003	*10*	397.84	397.78	0.06
Aluminum	A004	*13*	397.79	397.74	0.05
Aluminum	A005	*16*	398.10	398.06	0.04
Aluminum	A006	*19*	397.10	397.06	0.04
Aluminum	A007	*22*	397.74	397.71	0.03
Aluminum	A008	*25*	396.90	396.88	0.02
Aluminum	A009	*28*	397.20	397.16	0.04
Aluminum	A010	*31*	397.74	397.71	0.03
Aluminum	A011	*34*	396.28	396.26	0.02
Aluminum	A012	*37*	396.82	396.80	0.02
Aluminum	A013	*40*	398.39	398.40	-0.01
Aluminum	A014	*43*	397.17	397.15	0.02
Aluminum	A015	*46*	397.50	397.45	0.05

3.4.2 XRD analysis

Figure 20 shows the aluminum coupons before and after Test T4. The aluminum coupons were very shiny silver before testing, but after testing were a shiny black. Figure 21 shows aluminum, galvanized steel, and zinc coupons at the start and end of Test T3. White scale can be seen on the galvanized steel coupons in Test T3 but not in Test T4. The black scale was also observed on aluminum coupons at the end of Tests T3 and T4, as shown in Figure 20. A sample of the black scale from a Test T4 aluminum coupon was scraped off and subjected to XRD analysis. The analysis shows that the sample of black scale is primarily aluminum (98.1%), as shown in Figure 22. The field of merit for this diffraction pattern's phase identification is 0.8 (FOM<1 indicates excellent accuracy). It is assumed that the sample powder prepared for XRD might have been mistreated and too aggressively scraped due to its very thin scale layer. Further analysis with XPS indicated that the scale layer thickness in Test T4 was only 2.9 nm. Therefore the XRD result might contain too much pure metallic aluminum, which is not actually present in the scale layer. Future research should employ greater care in sample preparation using XRD or another surface analysis tool such as XPS. Due to contamination of the XRD result, an additional surface analysis tool (XPS) was employed with selected samples from Tests T3 and T4; the results are presented in the following section.

Figure 20: Test T4 submerged aluminum coupons before (left) and after (right) testing.

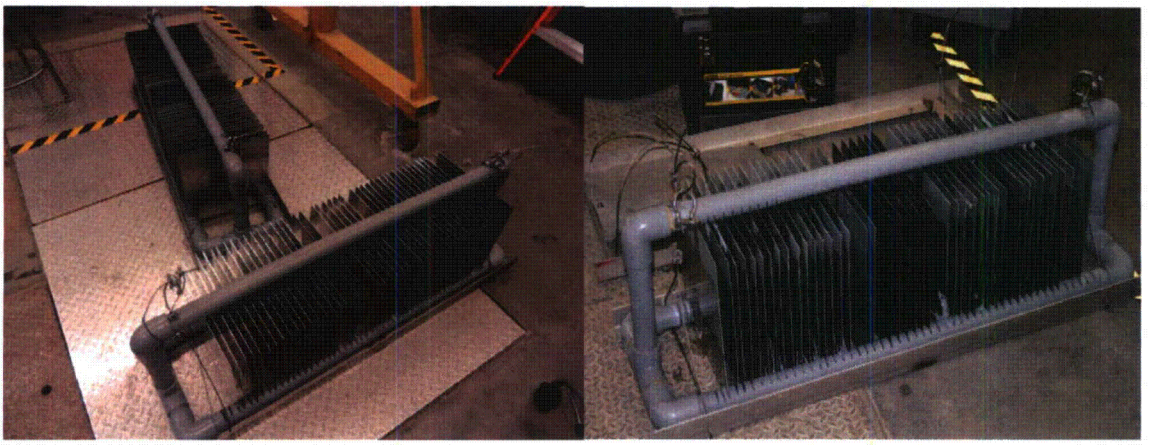

Figure 21: Test T3 submerged coupons before (left) and after (right) testing.

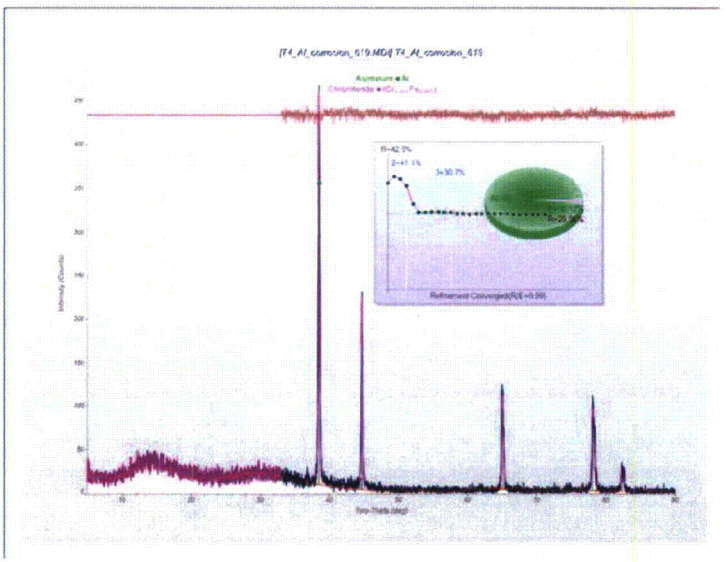

Figure 22: XRD result of corroded aluminum scale layer from Test T4.

3.4.3 XPS analysis

In order to investigate the surface characteristic of both post-tested aluminum coupons from Tests T3 and T4, representative samples of aluminum coupons were selected for X-ray photoelectron spectroscopy (XPS) analysis. The results can be seen in Figure 23. The blank sample of aluminum shows signal from metallic Al underneath aluminum oxide. For the Test T4 sample, a significant amount of metallic Al is present with an aluminum oxide layer, and some phosphate is detected as well. However, in the Test T3 sample, the thickness of aluminum oxide layer becomes much thicker than the alumina layer observed in Test T4 and no metallic Al signal was detected. Using different take-off-angles (TOA) in XPS, the oxide layer thickness can be calculated via the overlayer model using Angle-Resolved XPS [6].

With a help of XPS results using the overlayer model, the aluminum oxide layer in Test T4 was calculated to be 2.79 nm from the deference of two peaks in the XPS result, and the aluminum oxide layer in Test T3 could not be calculated due to the single peak, but the oxide layer is assumed to be at least thicker than 15 nm from XPS operation. It is also observed from XPS analysis that the oxygen concentration in the near surface area in Tests T3 and T4 is greater than the oxygen concentration in the surface of bare aluminum, which qualitatively explains the aluminum oxide layer build-up in the coupons in both tests. This hypothesis might explain why Test T3 has lower Al concentration ICP-OES result (2.5 mg/L) than that of Test T4 (5.1 mg/L). The thicker aluminum oxide layer cause less aluminum release into the solution. However, it is still not clear why Test T3 provided the effective kinetics for greater aluminum oxide layer growth than in Test T4. The presence of zinc in solution may be a factor.

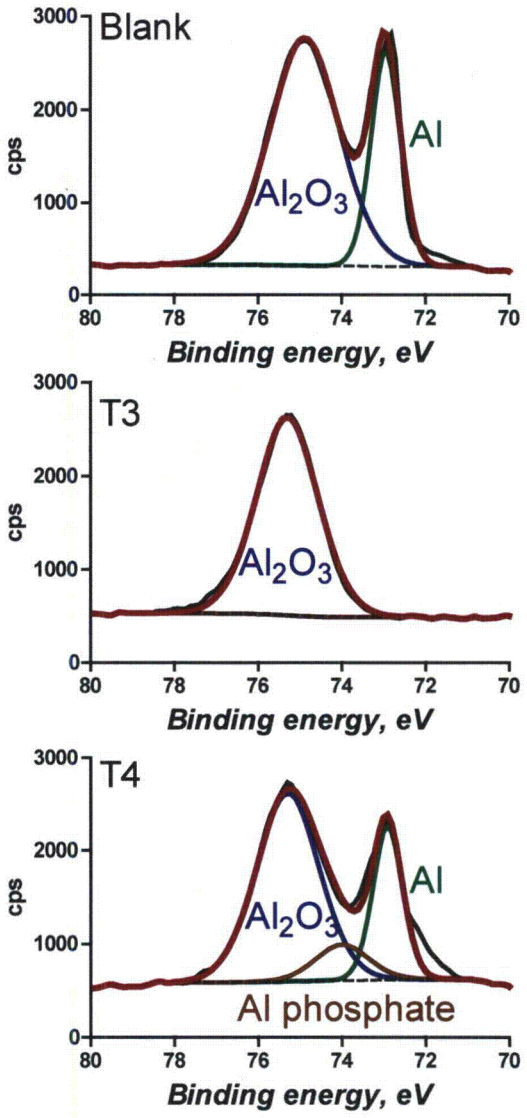

	Al 2p %	Zn 2p %	O 1s %	P 2p %	Ca 2p %	Cr 2p %
Bare Al	37.579	0.1064	61.754		0.5605	
T3 Al	14.2	0.3799	70.755	11.9	2.7656	
T4 Al	22.993		65.172	7.7574	0.1637	3.91425

Figure 23: XPS Al 2p spectra analysis result for Bare Al, Test T3 Al, and Test T4 Al.

3.4.4 SEM-EDS analysis

SEM analysis of the black layer of a Test T4 aluminum coupon was also performed. The coupon was cut into small pieces in preparation for this analysis, but the pieces were large enough to prevent any false readings due to the cutting procedure's possibly contaminating the edges of the sample. The results,

SEM-EDS, are shown in Figure 24. The results indicate the presence of an aluminum oxide or hydroxide layer on the coupon (i.e., ~27% oxygen and ~67% aluminum). Other elements detected in the EDS analysis could have been from dried tank solution that remained on the coupon. There was no evidence of particles on the Test T4 aluminum coupon.

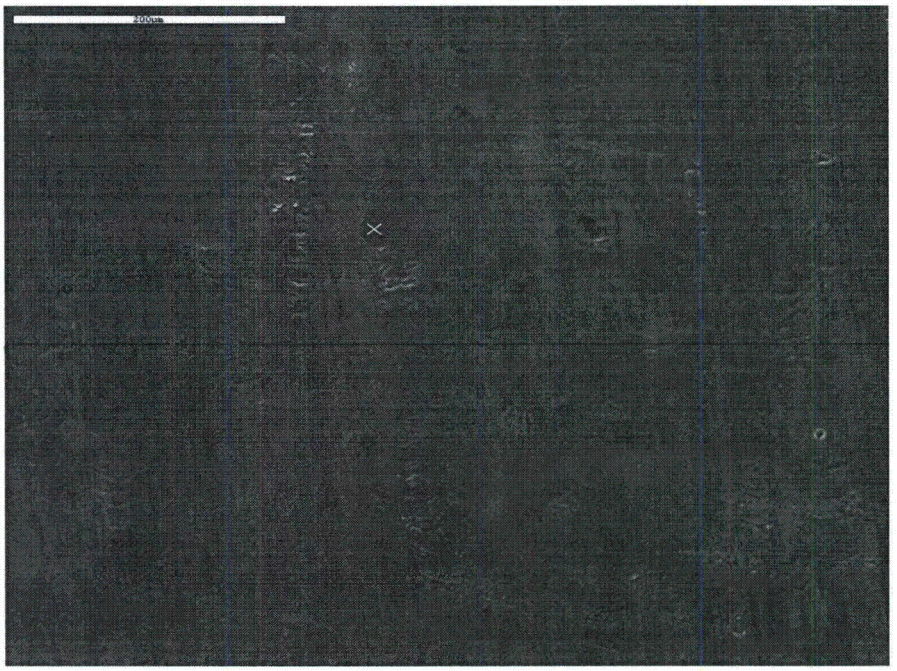

Elmt.	Element %	Sigma %	Atomic %
O	26.749	0.321	38.403
Na	0.601	0.072	0.600
Al	66.737	0.320	56.812
Si	0.211	0.068	0.173
P	4.420	0.129	3.278
Ca	1.282	0.084	0.735

Figure 24: SEM of aluminum coupon from Test T4, with EDS results of marked location.

SEM and EDS analysis was also performed on the Test T3 aluminum, zinc, and galvanized steel coupons. A sample SEM image with EDS results of marked location for each coupon can be seen in Figure 25, Figure 26, and Figure 27 for aluminum, zinc, and galvanized steel, respectively.

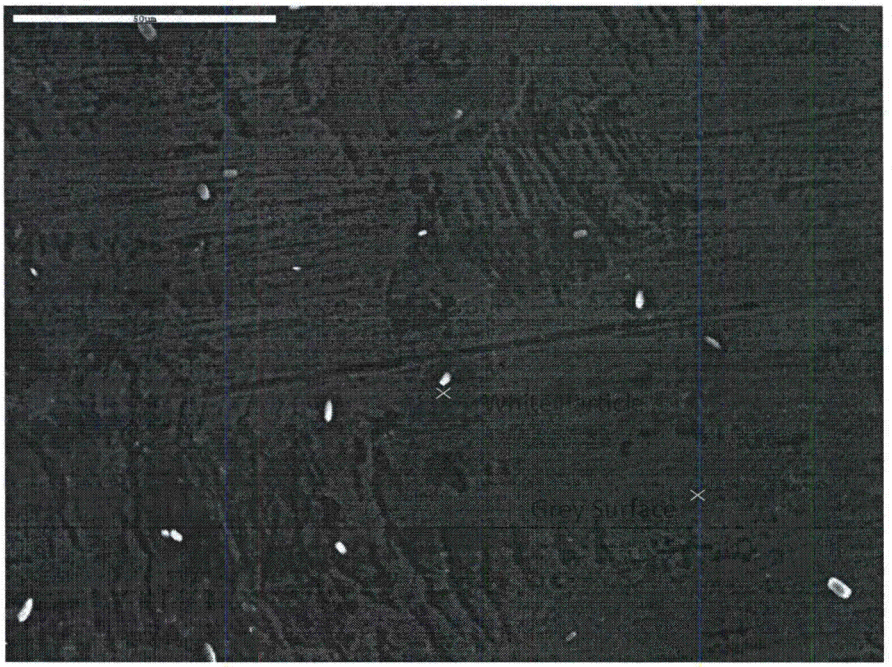

Grey Surface

Elmt.	Element %	Sigma %	Atomic %
O	17.337	0.265	26.553
Na	0.675	0.131	0.719
Al	75.763	0.511	68.805
P	3.360	0.115	2.658
Ca	0.807	0.092	0.493
Zn	2.059	0.559	0.772

White Particle

Elmt.	Element %	Sigma %	Atomic %
O	38.475	0.562	61.367
Na	4.158	0.430	4.616
Al	3.628	0.111	3.431
P	17.131	0.280	14.114
Ca	8.859	0.197	5.641
Zn	27.748	0.875	10.832

Figure 25: SEM of aluminum coupon from Test T3, with EDS results of marked locations (white particle and grey surface).

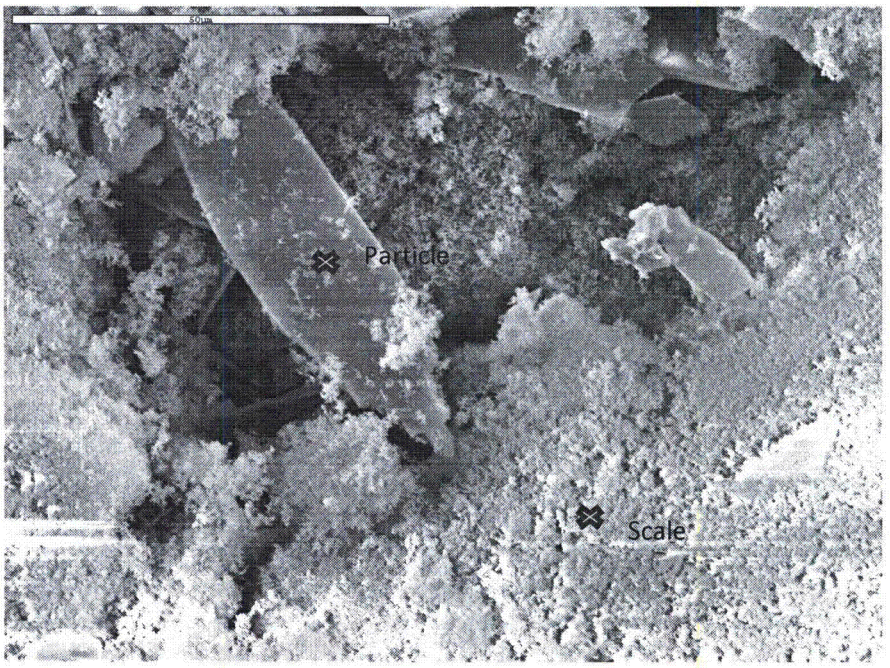

Particle

Elmt.	Element %	Sigma %	Atomic %
O	28.171	0.520	53.359
Na	7.042	0.559	9.282
P	14.230	0.285	13.922
Zn	50.556	0.835	23.436

Scale

Elmt.	Element %	Sigma %	Atomic %
O	30.122	0.534	55.697
Na	6.814	0.571	8.768
Al	0.264	0.077	0.289
P	13.584	0.269	12.974
Zn	49.215	0.825	22.272

Figure 26: SEM of zinc coupon from Test T3, with EDS results of marked locations (white particle and grey surface).

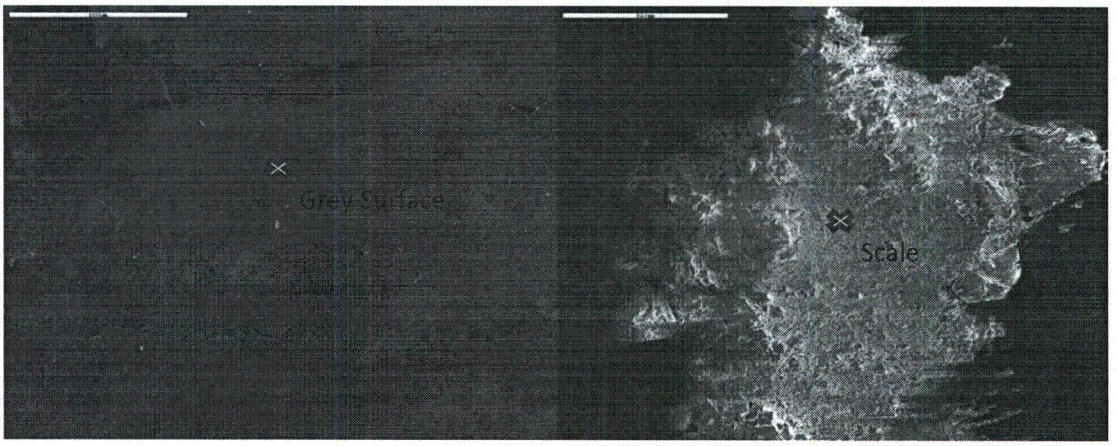

Grey Surface

Elmt.	Element %	Sigma %	Atomic %
O	4.645	0.193	15.085
Na	4.311	0.915	9.742
Al	1.964	0.110	3.782
P	0.675	0.097	1.133
Zn	88.404	0.891	70.258

Scale

Elmt.	Element %	Sigma %	Atomic %
O	30.925	0.531	55.776
Na	6.704	0.545	8.414
P	16.889	0.309	15.734
Zn	45.482	0.841	20.077

Figure 27: SEM of galvanized steel coupon from Test T3, with EDS results of marked locations (left image: clean part of sample, right image: white scale found on sample).

The EDS results for all three types of Test T3 coupons (Al, Zn, and galvanized steel) indicate the presence of a compound that may be zinc phosphate. This particle was not detected on any of aluminum coupons during Test T4. This is likely due to the presence of zinc material in Test T3 and its absence in Test T4. The presence of zinc material along with the solution chemistry, borated TSP solution, caused the formation of the zinc phosphate. In general, scattered zinc phosphate white particles were found in aluminum coupons in Test T3, and no zinc phosphate was found in aluminum coupons in Test T4 from the SEM-EDS analysis. Many zinc phosphate white particles and much scale was observed on both zinc and galvanized steel coupons in Test T3.

SEM-EDS analysis was also performed on samples from the fiber beds of Tests T3 and T4. An SEM image of the fiber beds in columns 1 and 3 of Test T4 can be seen in Figure 28, which indicates that the fiber bed of Column 1 in T4 shows much less deposited particulate than found in Column 3. This may explain

why Column 3 in Test T4 experienced a greater head loss than Column 1, as shown in Figure 18. The amount of particles present is expected to be a key factor in the amount of head loss experienced across a fiberglass bed.

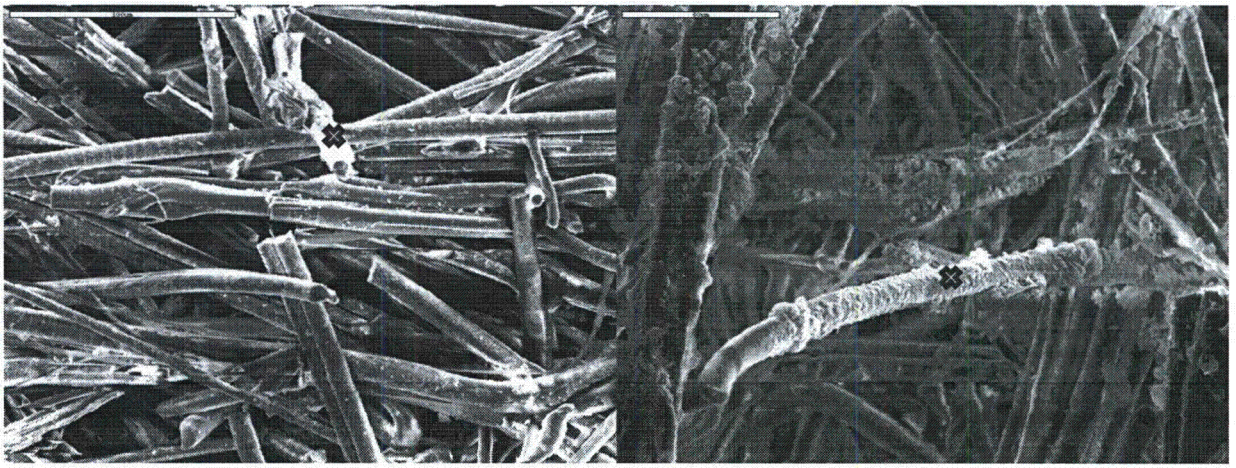

Scale

Elmt.	Element %	Sigma %	Atomic %
O	16.77	1.69	36.72
Na	3.04	0.75	4.63
Al	3.83	0.64	4.97
Si	4.65	0.57	5.80
P	3.21	0.90	3.63
Ca	5.26	1.03	4.60
Fe	63.25	2.52	39.66

Scale

Elmt.	Element %	Sigma %	Atomic %
O	51.62	1.00	67.67
Al	13.84	0.47	10.76
Si	1.07	0.20	0.80
P	21.16	0.77	14.33
Ca	12.31	0.62	6.44

Figure 28: SEM images of fiber bed in Column 1 and Column 3 in Test T4 with EDS results of marked location.

Based on EDS results, the particles found in the fiberglass beds of Test T4 appear to be a mixture of solution chemistry, sodium and phosphorous, fiberglass (Si), and metals found in the tank solution.

An SEM analysis of fiber bed of Column 1 in Test T3 can be seen in Figure 29, which shows that the particulate found on the fiber is quite different from that found on Test T4 fiber. Particulates in Test T4 appear to have been deposited on the fiber bed surface, whereas particulates in Test T3 appear stuck in the fiber bed pore region with a different structure layout. This might be explained by the particle size analysis. The average particle size at the beginning of Test T3 was around 1900 nm, which is 5 times larger than the average particle size at the beginning of Test T4 (i.e., around 350 nm). The larger particle in Test T3 may have been caught into the fiber bed at the beginning of test and brought about increased head loss on Days 1 and 2. This is consistent with the hypothesis that the zinc source effect on the normalized head loss increase at the beginning of Test T3. The EDS analysis for the marked location indicates that the particulate on the Test T3 fiber bed may contain a zinc phosphate compound. Zinc plates were not used in Test T4, which is why zinc phosphate compound was not found on Test T4 fiber.

Scale

Elmt.	Element %	Sigma %	Atomic %
O	12.16	0.80	29.45
Al	2.03	0.23	2.91
Si	2.13	0.20	2.94
P	14.77	0.84	18.48
Ca	14.41	0.80	13.93
Zn	54.50	2.08	32.30

Figure 29: SEM images of fiber bed in Column 1 in Test T3 with EDS results of marked location.

3.5 Flow Sweep Test

A flow sweep test was performed at the conclusion of Test T4 to develop a better understanding of the mechanical response of the fiber beds to varying flow conditions (approach velocities). Following a measurement of constant head loss, the velocity to each column was stepped up by an incremental value. Once the head loss was again stable and had been stable for a few minutes, the velocity was increased once again by the same amount. The process was repeated until sufficient data had been gathered. The final incremental approach velocities used were 0.010, 0.022, 0.044, 0.060, and 0.10 ft/s.

Columns 1 and 3 contained the blender-processed debris beds. In the past, the blender-processed debris beds have shown erratic mechanical behavior and repeatability. Test T4 was no exception; with the blender-processed debris beds, the head loss increased dramatically even though very little particulate

matter or corrosion products were present in the circulating solution. The flow sweep test with the blender-processed debris beds also exhibited this unpredictability. The results of the flow sweep test for Column 1 are shown in Figure 30 and Figure 31. As expected, head loss increased with the initial increase in approach velocity. After the first increment, from 0.020 to 0.060 ft/s, the head loss would spike and then settle back down to about 27 inches. This repetition continued until reaching an approach velocity of 0.10 ft/s, at which time the head loss again behaved as it had for the first velocity step. The expected linear relationship between head loss and approach velocity did not occur for the blender-processed beds, as shown in Figure 31. One explanation for the different behaviors could lie within the physical properties of the blender-processed bed itself. The shards of fiberglass that compose the blender-processed bed are very small, almost soupy particles. It is postulated that head loss increases when these fibers come together and clog the holes in the support screen. The fiber bed itself does not cause head loss on the macro scale, but it induces clogging of the small screen holes that appears to cause head loss. If this is the case, then the increasing and dropping off of head loss shown in Figure 30 could be the clogged hole on the screen becoming unclogged by the fiber breaking through the screen. This phenomenon could be occurring all over the screen. There may be a limiting factor on the head loss through the blender-processed bed locally at the screen holes that is controlled by the static friction between fiberglass particles and the surface of the screen.

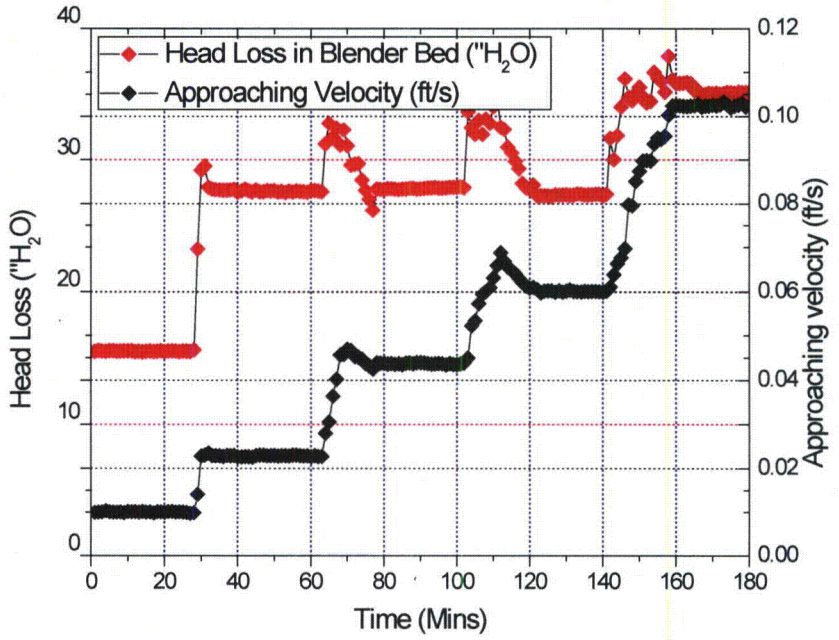

Figure 30: Flow sweep test with blender-processed bed (approaching velocities: 0.010, 0.022, 0.044, 0.6, and 0.10 ft/s).

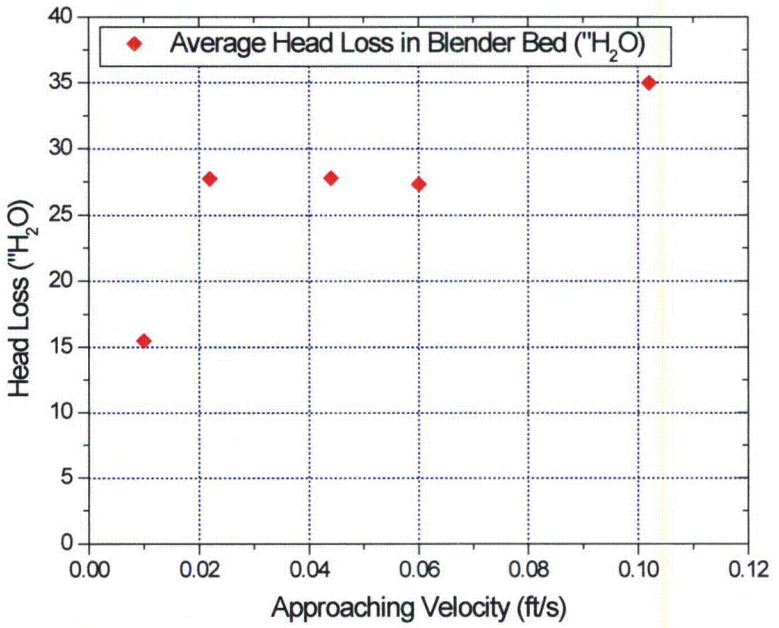

Figure 31: Average head loss with varying approaching velocities in blender-processed bed.

Column 2 contained the NEI-processed debris bed for Test T4. The bed's head loss increased linearly with the increase in approach velocity, as shown in Figure 32 and Figure 33. This bed apparently did not exhibit the local head loss at the screen holes that was found in the blender-processed debris bed. Since NEI fibers have a characteristic length much greater than that of the diameter of the holes in the column screens, they can lie across the screen and not fill the holes. The bed exhibits behaviors that indicate that head loss is a function of approach velocity as predicted by equations for head loss through a porous bed.

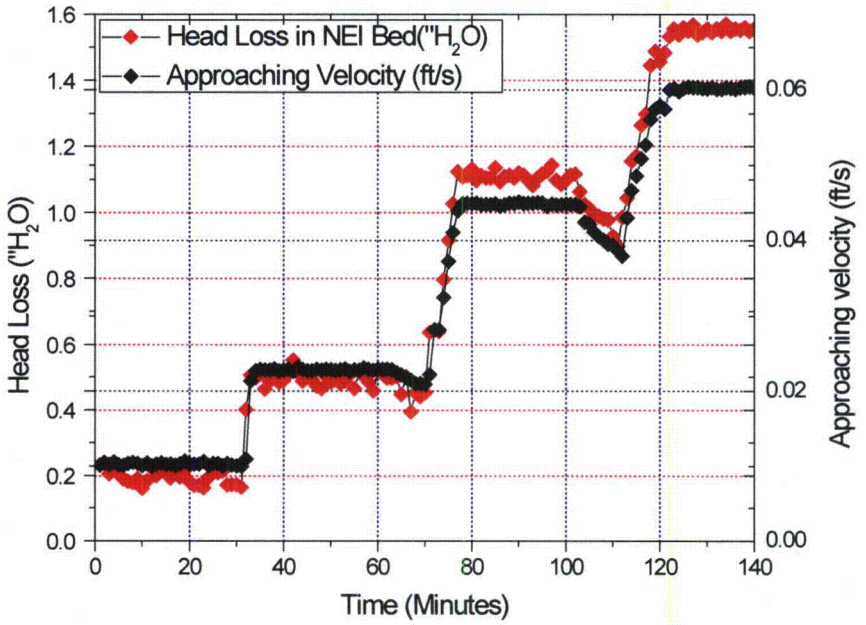

Figure 32: Flow sweep test with NEI bed (approaching velocities: 0.010, 0.022, 0.044, 0.60 and 0.10 ft/s).

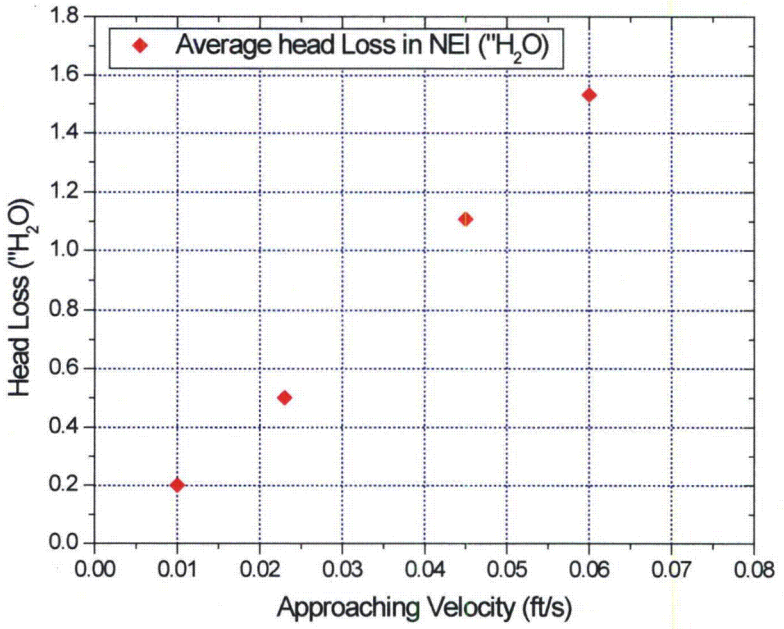

Figure 33: Average head loss with varying approaching velocity in NEI bed.

4.0 Summary and Conclusions

The observations for Tests T3 and T4 are summarized below.

1. The head loss increased across all three columns with different trends during the 10-day tests. Generally, the blender-processed debris beds produced significantly higher head loss than did NEI-processed debris beds.
2. The head loss in Column 1 (blender-processed debris bed) started increasing rapidly from the beginning of Test T3, decreased slightly until Day 6 due to bed stabilization, and again increased after Day 6. The column was shut down at Day 8 upon reaching the target maximum head loss condition. In Test T4, the head loss in Column 1 started increasing from Day 4, and then the rate increased as the solution turbidity increased. The rate of increase slowed during Days 11 and 12 as the turbidity leveled off.
3. The head loss in Column 2 in Tests T3 and T4 (NEI-processed debris bed) increased over the 10-day tests, but the final head loss was below 1 inch in both cases.
4. The head loss trend in Column 3 in Test T3 was very similar to the trend in Column 1. In Test T4, the head loss in Column 3 started increasing during Day 3.5, started to level off by Day 6, and reached the highest value of any of the three columns in Test T4. Upon reaching the target maximum head loss condition, Column 3 was shut down at Day 7.
5. The aluminum concentrations reached a plateau by the second day (2.6 mg/L for Test T3 and 5.1 mg/L for Test T4), stayed at approximately that concentration until Day 6, and then decreased gradually as the tank temperature decreased. Some variability (0.1 to 0.2 mg/L) from Day 2 to Day 6 was observed. The declining aluminum concentration after Day 6 indicates aluminum being removed from solution, possibly by being filtered through the debris beds after becoming supersaturated and precipitating.
6. The calcium concentrations increased to 1.3 mg/L for Test T3 and 2.1 mg/L for Test T4 by Day 6, and then fluctuated over the remaining testing period for both tests. Variability in calcium concentrations may be due to the fact that the concentrations were below the laboratory's normal reporting limit.
7. The silicon concentrations in Tests T3 and T4 gradually increased to 13 mg/L and 16 mg/L by Day 8, respectively, and plateaued over the remaining test period.
8. For calcium, aluminum, and silicon, filtered and total concentrations were nearly identical throughout the entire tests. The filtered samples were put through a 0.1 μm filter prior to analysis, thus indicating that no particles containing measurable amounts of Al, Ca, or Si larger than 0.1 μm were present in the solution.
9. Turbidity measurements in Test T3 rose to a peak of 2.6 NTU on the first day. This peak lasted only for 5 hours and declined rapidly, such that by the end of the first day the turbidity was below 0.5 NTU and gradually decreased to less 0.1 NTU by Day 6. After Day 7, the turbidity increased gradually to 0.5 NTU, while tank temperature decreased until the end of Test T3.
10. Turbidity measurements in Test T4 began at a peak of approximately 0.4 NTU and gradually decreased to about 0.1 NTU by Day 6. After Day 7, the turbidity increased gradually to 0.7

NTU, while the tank temperature went down, during the time when the aluminum concentration was decreasing. After 10 days, when tank temperature was maintained at 35°C for an additional 2 days, the tank turbidity leveled off at 0.7 NTU.

11. The zinc concentration in Test T3 started at 1.5 mg/L for total zinc and 0.44 mg/L for filtered zinc. Total zinc declined rapidly, such that both total and filtered were 0.3 mg/L after 1 day and declined slowly to 0.2 mg/L throughout the test. The results indicate the presence of zinc particles at the beginning of the test that were removed within the first day.
12. The combination of decreasing aluminum concentration and increasing turbidity suggests that aluminum precipitates of a range of sizes were formed. Larger particles were removed from solution, contributing to a reduction in the aluminum concentration and the increase in head loss in the blender-processed beds, while smaller particles (<0.1 μm) stayed in solution and contributed to the increase in turbidity.
13. The submerged aluminum coupons in Tests T3 and T4 turned black, indicating the presence of a scale layer that may have led to passivation of the surface. In Test T3, white scale was formed and deposited on most of the galvanized steel and some of zinc coupons. Based on the XRD result for both tests' aluminum coupons, the black scale was identified as primarily an aluminum oxide layer, and white scale found in most T3 testing was identified as zinc phosphate compound from the EDS analysis.
14. SEM images on the fiber bed in Tests T3 and T4 led to the conclusion that the amount of particles present may play a key role in the amount of head loss experienced across a fiberglass bed.
15. XPS results with the overlayer model suggest that the aluminum oxide layer of Test T4 is thinner that of Test T3. This might couple with the ICP-OES result in aluminum concentration in solution. The thicker oxide layer in Test T3 (>15 nm) would cause less aluminum concentration in solution (2.5 mg/L), and the thinner oxide layer in Test T4 (2.9 nm) would cause more aluminum concentration in solution (5.1 mg/L). The difference in oxide layer growth might come from the presence of zinc in the solution.
16. The sweep test supports the contention that head loss in the blender-processed debris beds do not vary linearly with approach velocity, and that it does vary linearly with approach velocity in the NEI-processed debris beds.
17. The turbidity, particle size, zeta potential, and metals concentrations are consistent with each other. At the beginning of Test T3, zinc particles were formed, as indicated by the difference between the filtered and total zinc concentrations. These particles had an average size of 1.9 μm and zeta potential near zero, which facilitated their removal from solution. After the zinc particles were removed, the average size of the remaining particles dropped below 0.2 μm and the zeta potential of the remaining particles was between -25 and -35 mV, indicating much smaller and more stable particles that would be harder to remove from solution. After the initial particle removal in Test T3, turbidity dropped gradually during the next 5 to 6 days in Test T3 as well as in Test T4, indicating the slow removal of latent debris particles of unknown composition. This slow drop in turbidity was also observed in previous 30-day tests. After Day 7, the turbidity increased in both tests,

indicating the formation of particles that remained in solution. The similarity between filtered and total metals concentrations indicates that particles are smaller than the filtration size (0.1 μm). The particle size data also indicate that the particles were smaller than 0.1 μm. The zeta potential data indicate that these particles would be stable and would not have a tendency to flocculate and form larger particles.

18. When all head loss results are considered in aggregate, neither the NEI-processed nor the blender-processed beds are an unquestionable detector of chemical effects. The NEI-processed had generally low head loss over the duration of both tests, with normalized head loss below 1 inch. The blender-processed beds are highly sensitive to zinc particles that entered the solution at the beginning of Test T3, aluminum precipitates that formed later in both tests, latent debris, and possibly other factors. As turbidity leveled off late in Test T4, the head loss in Column 1 also started to level off. However, the blender-processed beds in Test T4 also had a period of increasing head loss between Days 3.5 and 6 that is difficult to definitively attribute to either zinc particle or aluminum precipitates with certainty. The increasing head loss during that period may have been due to continued filtration of latent debris, early onset of precipitation, or other perturbations to the system. Thus, it is not possible to attribute an increase in head loss in the blender-processed beds to chemical effects, without correlation with other types of data (aluminum concentrations, turbidity, etc.). However, because the blender-processed beds are so sensitive, the absence of an increase in head loss can be used as an indication of the absence of chemical effects.
19. The results of these tests support the conclusion that chemical effects did not occur in the CHLE MBLOCA (T1) or LBLOCA (T2) tests conducted in 2012. The concentrations of aluminum in those tests were more than an order of magnitude lower than the concentrations observed in these tests, and were below the concentrations at which precipitation started occurring in these tests. In fact, when precipitation was complete at the end of 10 days in these tests, the remaining aluminum in solution was considerably higher than the concentrations of aluminum in T1 and T2. Furthermore, the turbidity declined gradually over the duration of those tests and did not show the signature increase that indicates precipitation. Comparison to the aluminum solubility map developed by Argonne National Lab is consistent with the occurrence of precipitation in Tests T3 and T4 but not in Tests T1 and T2. Finally, the blender-processed beds that were installed in the columns at the end of the 30-day tests did not exhibit a rapid increase in head loss, and evidence from the current tests suggests that traces of particles or precipitates should have caused a significant increase in head loss if precipitates had been present.

5.0 References

1. UNM, CHLE-012, *T1 MBLOCA test report 2012*, University of New Mexico: Albuquerque, NM.
2. UNM, CHLE-014, *T2 LBLOCA test report 2012*, University of New Mexico: Albuquerque, NM.
3. UNM, CHLE-017, *Tests to assess chemical precipitate formation*, University of New Mexico: Albuquerque, NM.

4. Lane, A.E. et al., *Evaluation of post-accident chemical effects in containment sump fluids to support GSI-191*, 2006, Westinghouse Electric Company: Pittsburgh, PA.
5. Bahn, C.B., Kasza, K.E., Shack, W.J., Natesan, K., and Klein, P. Evaluation of precipitation used in strainer head loss testing: Part III. Long-term aluminum hydroxide precipitation tests in borated water, *Nuclear Engineering and Design*, vol. 241, pp. 1914-1925, 2011.
6. Jablonski, A., Zemek, J., Overlayer thickness determination by XPS using the multiline approach, *Surface and Interface Analysis,* vol. 41, issue 3, pp. 193-204, 2009..
7. Trethewey, K.R., Chamberlain, J., *Corrosion for students of science and engineering*, Longman Scientific & Technical, Hong Kong, 1988, p. 281.